

THE EFFECT OF AUSTEMPERING PARAMETERS ON IMPACT AND  
FRACTURE TOUGHNESS OF DIN 35NiCrMoV12.5 GUN BARREL STEEL

A THESIS SUBMITTED TO  
THE GRADUATE SCHOOL OF NATURAL AND APPLIED SCIENCES  
OF  
MIDDLE EAST TECHNICAL UNIVERSITY

BY

ENGİN AKSU

IN PARTIAL FULFILLMENT OF THE REQUIREMENTS  
FOR  
THE DEGREE OF MASTER OF SCIENCE  
IN  
METALLURGICAL AND MATERIALS ENGINEERING

JULY 2005

Approval of the Graduate School of Natural and Applied Sciences

---

Prof. Dr. Canan Özgen  
Director

I certify that this thesis satisfies all the requirements as a thesis for the degree of Master of Science.

---

Prof. Dr. Tayfur Öztürk  
Head of Department

This is to certify that we have read this thesis and that in our opinion it is fully adequate, in scope and quality, as a thesis for the degree of Master of Science.

---

Prof. Dr. Haluk Atala  
Supervisor

**Examining Committee Members**

Prof. Dr. Ömer Anlağan (TÜBİTAK) \_\_\_\_\_

Prof. Dr. Haluk Atala (METU, METE) \_\_\_\_\_

Prof. Dr. Tayfur Öztürk (METU, METE) \_\_\_\_\_

Prof. Dr. Şakir Bor (METU, METE) \_\_\_\_\_

Prof. Dr. Rıza Gürbüz (METU, METE) \_\_\_\_\_

**I hereby declare that all information in this document has been obtained and presented in accordance with academic rules and ethical conduct. I also declare that, as required by these rules and conduct, I have fully cited and referenced all material and results that are not original to this work.**

Name, Last name :Engin Aksu

Signature :

## **ABSTRACT**

### **THE EFFECT OF AUSTEMPERING PARAMETERS ON IMPACT AND FRACTURE TOUGHNESS OF DIN 35NiCrMoV12.5 GUN BARREL STEEL**

AKSU, Engin

M.S., Department of Metallurgical and Materials Engineering

Supervisor: Prof. Dr. Haluk Atala

July 2005, 84 pages

In this study the effects of different austempering times and temperatures on impact toughness, hardness and fracture toughness properties of 35NiCrMoV12.5 gun barrel steel are investigated. 300 °C, 325 °C and 350 °C were chosen as austempering temperatures. Isothermal holding times at these temperatures were chosen as 1 minute, 10 minutes, 1 hour and 10 hours. It was found that, 350 °C being an exception, austempering temperature and impact toughness has an inverse relationship and impact toughness increases as isothermal holding time increases. However this behavior is valid until some point. Prolonged transformation times causes toughness to decrease. Hardness measurements revealed that, as isothermal holding time increases, hardness decreases. In order to compare the mechanical properties obtained by austempering with

that of conventional cooling and tempering, 400 °C was chosen as the tempering temperature and applied to both charpy impact and fracture toughness specimens. It was found that conventional cooling and tempering produced tougher structures. Size of the fracture toughness specimens might have caused an undesired situation such as incomplete transformation to bainite. Optical and scanning electron microscopy was used in order to analyze the microstructures obtained after each treatment. It was observed that the majority of the morphologies occurred is lower bainite. On the other hand, martensitic structures were observed almost at every temperature.

**Keywords:** Austempering, Bainite, Gun Barrel, Toughness

## ÖZ

### **DIN 35NiCrMoV12.5 NAMLU ÇELİĞİNDE ÖSTEMPERLEME PARAMETRELERİNİN DARBE VE KIRILMA TOKLUĞU ÜZERİNE ETKİLERİ**

AKSU, Engin

Yüksek Lisans, Metalürji ve Malzeme Mühendisliği Bölümü

Tez Danışmanı: Prof. Dr. Haluk Atala

Temmuz 2005, 84 sayfa

Bu çalışmada, değişik östemperleme zaman ve sıcaklıklarının 35NiCrMoV12.5 namlu çeliğinde darbe tokluğu, sertlik ve kırılma tokluğu özellikleri üzerine etkileri araştırılmıştır. 300 °C, 325 °C ve 350 °C ler östemperleme sıcaklıkları olarak seçilmiştir. Bu sıcaklıklardaki izotermal dönüşüm süreleri ise 1 dakika, 10 dakika, 1 saat ve 10 saat olarak seçilmiştir. 350 °C istisna olmak üzere, östemperleme sıcaklığı ile kırılma tokluğu arasında ters orantı olduğu ve izotermal dönüşüm süresi arttıkça kırılma tokluğunun arttığı bulunmuştur. Ancak bu durum belirli bir süreye kadar geçerlidir. Uzun süreli dönüşüm tokluğun düşmesine neden olmuştur. Sertlik ölçümleri göstermiştir ki, izotermal dönüşüm süresi arttıkça sertlik düşmüştür. Östemperleme ile elde edilen

mekanik özelliklerin konvansiyonel soğutma ve menevişleme ile elde edilenlerle karşılaştırılması için, 400 °C menevişleme sıcaklığı olarak seçilip, hem darbe tokluğu hem de kırılma tokluğu numunelerine uygulanmıştır. Konvansiyonel soğutma ve menevişlemenin daha tok yapılar oluşturduğu bulunmuştur. Kırılma tokluğu numunelerinin boyutu beynite tam dönüşememe gibi birtakım arzu edilmeyen sonuçların elde edilmesine neden olmuş olabilir. Optik ve tarama elektron mikroskopları elde edilen mikro yapıların analiz edilmesinde kullanılmıştır. Genellikle elde edilen yapıların alt beynit olduğu gözlenmiştir. Ancak, hemen her sıcaklıkta martensitli yapılar da gözlenmiştir.

Anahtar kelimeler: Östemperleme, Beynit, Namlu Çeliği, Tokluk

To My Parents, Didem, and Gary

## ACKNOWLEDGEMENTS

I would like to express my deepest gratitude to my supervisor, Prof. Dr. Haluk Atala, for his guidance, advice, criticism, encouragement and insight throughout the research.

I am also grateful to Prof. Dr. Rıza Gürbüz for his suggestions and comments throughout the mechanical test steps of this study.

I would also like to appreciate Mr. Gündüz Güler, deputy factory manager of MKE Kirikkale Heavy Weapon and Steel Factory for his help and support regarding materials supply.

Special thanks to my family, Didem Evcimen and Gary L. Buterbaugh for their support and never ending encouragement.

Finally, thanks to all the technical staff of the Metallurgical and Materials Engineering Department for their help during this study.

## TABLE OF CONTENTS

ABSTRACT.....	iv
ÖZ.....	vi
DEDICATION.....	viii
ACKNOWLEDGEMENTS.....	ix
TABLE OF CONTENTS.....	x
LIST OF TABLES.....	xii
LIST OF FIGURES.....	xiii
LIST OF EQUATIONS.....	xvi
CHAPTER	
1. INTRODUCTION.....	1
2. AUSTEMPERING.....	3
3. BAINITE IN STEELS.....	7
3.1 Definition.....	7
3.2 Reaction Mechanism.....	8
3.3 Upper and Lower Bainite.....	10
3.4 Mechanical Properties.....	13
3.4.1 Impact Toughness.....	13
3.4.2 Fracture Toughness.....	15
3.4.2.1 Cleavage Fracture Path.....	18
3.4.3 Hardness.....	20

4. LITERATURE REVIEW.....	22
5. EXPERIMENTAL PROCEDURE.....	28
5.1 Chemical Composition.....	30
5.2 Sampling of Specimens 20 & 30.....	30
5.3 Heat Treatment Pre-study.....	31
5.4 Heat Treatment Procedure.....	34
5.5 Notched Bar Impact Test (Charpy).....	37
5.6 Hardness Test.....	39
5.7 Fracture Toughness Test.....	39
5.8 Optical Microscopy.....	41
5.9 Electron Microscopy.....	41
6. RESULTS.....	42
6.1 Charpy Impact Test.....	42
6.2 Hardness Test.....	46
6.3 Fracture Toughness Test.....	48
7. DISCUSSION.....	50
7.1 Charpy Impact Test.....	50
7.2 Hardness Test.....	55
7.3 Fracture Toughness Test.....	57
7.4 Microstructural Features.....	59
8. CONCLUSION.....	76
REFERENCES.....	78
APPENDIX.....	82

## LIST OF TABLES

2.1 Comparison of Austempering and Conventional Quenching and Tempering.....	6
2.2 Comparison of Austempering and Conventional Quenching and Tempering.....	6
5.1 Chemical composition of the specimens used.....	30
5.2 Austempering temperatures and times investigated in the study.....	34
5.3 Conventional quenching and tempering temperatures and corresponding hardness values.....	36

## LIST OF FIGURES

2.1 Austempering heat treatment cycle.....	4
3.1 a) Bainite obtained by isothermal transformation at 290 °C.....	7
3.1 b) Bainite obtained by isothermal transformation at 180 °C.....	7
3.2 Hypothetical TTT diagram.....	9
3.3 Atomic comparison of displacive and reconstructive transformation.....	9
3.4 Upper and Lower Bainite.....	10
3.5 High resolution atomic-force microscope plot.....	12
3.6 Schematic illustration of impact transition curves.....	14
3.7 a) $K_{IC}$ values plotted against corresponding values of the stress.....	17
3.7 b) Values plotted against test temperatures.....	17
3.7 c) Carbide size distributions obtained from martensitic and bainitic microstructures.....	17
3.8 Schematic Illustration of Crack Propagation in Fully Bainitic Microstructures.....	18
3.9 Packets that form in prior austenite grain.....	19
3.10 Schematic illustration of crack propagation in bainitic-martensitic mixed microstructures.....	20
3.11 Variation in hardness as a function of the isothermal transformation temperature..	21
5.1 Specimen shape and dimensions.....	28
5.2 Schematic illustration of the coding scheme and Charpy samples extracted from the original specimen.....	29
5.3 Illustration of the coding technique.....	31
5.4 AISI 4340 Time-Temperature-Transformation Diagram.....	32
5.5 Austempering procedure applied.....	35

5.6 The experimental setup.....	35
5.7 The standard charpy test specimen.....	37
5.8 Illustration of the charpy impact test and the direction of the force applied.....	37
5.9 Charpy impact bar samples prepared after heat treatment.....	38
5.10 Charpy impact test machine used.....	38
5.11 Hardness test machine.....	39
5.12 Standard SENB test specimen.....	39
5.13 MTS Testing machine in operation during pre-cracking the specimens.....	40
5.14 Also Laboratory Machine used to fracture the specimens until failure.....	40
5.15 Optical microscope used.....	41
6.1 Impact Toughness values of the specimens which were austempered at 300 °C.....	43
6.2 Impact Toughness values of the specimens which were austempered at 325 °C.....	44
6.3 Impact Toughness values of the specimens which were austempered at 350 °C.....	45
6.4 Hardness values of the specimens which were austempered at 300 °C.....	47
6.5 Hardness values of the specimens which were austempered at 325 °C.....	47
6.6 Hardness values of the specimens which were austempered at 350 °C.....	48
7.1 Comparison of different austempering temperatures with respect to impact toughness values obtained at different transformation times.....	52
7.2 Comparison of different austempering times with respect to impact toughness values obtained at different transformation temperatures.....	53
7.3 Comparison of the austempering temperatures with respect to hardness values obtained at different transformation times.....	56
7.4 Comparison of the austempering times with respect to hardness values obtained at different transformation temperatures.....	56
7.5 Comparison of the fracture toughness values of austempered and conventionally quenched and tempered specimens.....	57
7.6 Water quenched, 100% Martensite samples.....	61
7.7 Microstructure obtained after austempering at 300 °C for 1 min.....	62
7.8 Microstructure obtained after austempering at 300 °C for 1 min.....	63
7.9 Microstructure obtained after austempering at 300 °C for 10 min.....	64
7.10 Microstructure obtained after austempering at 300 °C for 10 hours.....	65

7.11 Microstructure obtained after austempering at 300 °C for 10 hours.....	65
7.12 Microstructure obtained after austempering at 325 °C for 1 min.....	66
7.13 Microstructure obtained after austempering at 325 °C for 1 min.....	67
7.14 Microstructure obtained after austempering at 325 °C for 1 min.....	68
7.15 Microstructure obtained after austempering at 325 °C for 10 minutes.....	69
7.16 Microstructure obtained after austempering at 325 °C for 10 hours.....	70
7.17 Microstructure obtained after austempering at 325 °C for 10 hours.....	70
7.18 Microstructure obtained after austempering at 350 °C for 1 minute.....	71
7.19 Microstructure obtained after austempering at 350 °C for 1 minute.....	72
7.20 Microstructure obtained after austempering at 350 °C for 1 minute.....	72
7.21 Microstructure obtained after austempering at 350 °C for 1 minute.....	73
7.22 Microstructure obtained after austempering at 350 °C for 10 hours.....	74
7.23 Microstructure obtained after austempering at 350 °C for 10 hours.....	74
7.24 Microstructure obtained after austempering at 350 °C for 10 hours.....	75

## LIST OF EQUATIONS

3.1 Plain strain fracture toughness associated with corresponding critical stress and distance.....	15
5.1 Empirical Martensite start temperature equation.....	33
5.2 Empirical Martensite start temperature equation.....	33
5.3 Empirical Martensite start temperature equation.....	33

## CHAPTER 1

### INTRODUCTION

The medium carbon, high alloy steels such as DIN 35NiCrMoV12.5 are heavily used in military applications in the production of barrels, rifles, tank guns etc. due to their superior mechanical properties. Especially those parts which require high impact resistance and hardness are mainly manufactured from the aforesaid steels.

The importance of toughness for barrel materials is that, the gun barrel should resist sudden and unstable cracks, thus fractures, which occur without any warning in brittle materials. So the minimization of distortion and obtaining a tougher steel needed to be obtained, which was possible by heat treatment.

Such required mechanical properties for barrels were obtained by utilizing a special treatment called austempering which came to be used in the production of gun parts during World War II. It was found that the process resulted in low distortion and parts produced were tougher than the quenched and tempered components they replaced. However, the equipment used was very inefficient and the treatment was still in its infancy. By the 1950's the austempering process was routinely applied to steel and malleable iron parts.

The difference between conventional treatment and austempering is their treatment cycle. During austempering, the part is first austenitized, and then transformed at a constant temperature higher than  $M_s$  and lower than the nose region of the appropriate time-temperature-transformation diagram. However, during the conventional treatment, tempering is required after austenitizing and quenching the part.

The object of austempering is to produce bainite, which displays improved combinations of toughness and hardness when compared to martensite. Consequently, the reason why the austempering heat treatment produces superior mechanical properties is that the final product of the treatment is bainite rather than martensite, which occurs after conventional treatment.

In this study, the effect of austempering parameters (time and temperature) on mechanical properties related to gun parts are investigated.

## CHAPTER 2

### AUSTEMPERING

Austempering is an isothermal heat treatment alternative to conventional quenching and tempering, during which the steel is heated to the austenitic phase and then quenched to a temperature above martensite start ( $M_s$ ) with the aim of obtaining bainite instead of martensite [1].

In Metals Handbook [2] the austempering cycle is defined as follows:

- Heating the steel to a temperature within the austenitizing range, usually 790 to 870 °C (1450 to 1600 °F),
- Quenching in a bath maintained at a constant temperature, usually in the range of 260 to 400 °C (500 to 750 °F),
- Allowing the steel to transform isothermally to bainite in this bath,
- Cooling it to room temperature, usually in still air.

Figure 2.1 shows the austempering cycle.

On the other hand, the conventional heat treatment cycle differs from austempering in the second step where the steel is quenched drastically in a bath of oil or water, kept usually at room temperature, to yield the hard and brittle martensite. Next, the material is tempered at 170 °C to 600 °C to impart improved toughness to the material.

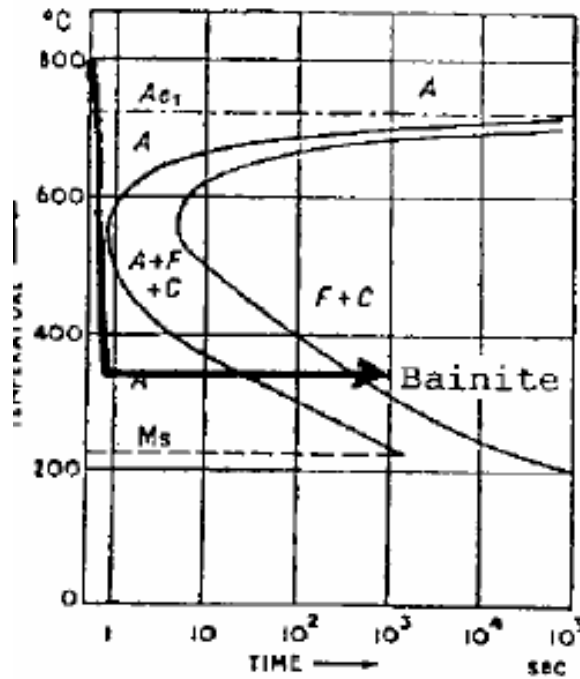


**Figure 2.1** Austempering heat treatment cycle (Ref. 3)

In some applications, the cost of austempering is much lower than that of conventional quenching and tempering. This situation is more likely for small parts which are treated in an automated set-up wherein conventional quenching and tempering comprise a three step operation – that is, austenitizing, quenching and tempering, whereas austempering requires only two processing steps. [2]

In conventional heat treatment, parts are quenched to room temperature, and martensite reaction begins immediately which is actually a “non-uniform phase transformation” due to inside and outside temperature differences in the quenched part. This non-uniformity causes distortion and tiny micro-cracks to appear which reduce the strength of the part.

However, during the austempering cycle, occurrence of bainite takes place over a longer period of time (many minutes or hours). This results in uniform growth, and a much stronger (less disturbed) microstructure.

To sum up; austempering is usually a preferred heat treatment especially to conventional quenching and tempering. This is mainly because the treatment offers:

- i) improved mechanical properties (particularly higher ductility or notch toughness at a given high hardness) [2]
- ii) a reduction in the likelihood of distortion and cracking which can occur in martensitic transformations [4]

In order to achieve true austempering, care must be taken in the following two steps [2]:

- i) The pace of cooling from the austenitizing temperature to the austempering temperature should be fast enough, so that transformation of austenite to higher temperature products is hindered. (complete avoidance of the nose of the TTT curve)
- ii) The austempering time should be long enough to ensure that full transformation to bainite is achieved.

The quenching media for austempering is usually molten salt. [2]

A quick comparison of a 5 mm diameter, 0.85% C plain carbon steel treated with both austempering and conventional quenching and tempering is shown below in Table 2.1. It can be seen that in austempered carbon steel parts, reduction in area is usually much higher: [2]

**Table 2.1** Comparison of Austempering and Conventional Quenching and Tempering for 5 mm diameter bars of 0.85% C plain carbon steel (Ref. 2)

	<b>Austempered</b>	<b>Quenched and Tempered</b>
<b>Tensile Strength (MPa)</b>	1780	1795
<b>Yield Strength (MPa)</b>	1450	1550
<b>Reduction in Area (%)</b>	45	28
<b>Hardness (HRC)</b>	50	50

Another comparison of austempering and conventional quenching and tempering for 0.74% C steel is as follows: [1]

**Table 2.2** Comparison of Austempering and Conventional Quenching and Tempering of a 0.74% C, 0.37% Mn, 0.145% Si, 0.039% S, 0.044% P steel. (Ref. 2)

	<b>Austempered</b>	<b>Quenched and Tempered</b>
<b>Hardness (HRC)</b>	50.4	50.2
<b>Ultimate Strength (ksi)</b>	282.7	246.7
<b>Yield Point (ksi)</b>	151.3	121.7
<b>Elongation, % in 6 inches</b>	1.9	0.3
<b>Reduction in area (%)</b>	34.5	0.7
<b>Impact (ft-lb)</b>	35.3	2.9

It can be seen that, the austempered steel displays better ductility and impact toughness than the same steel in the quenched and tempered condition.

As a result, austempering procedure helps minimization of residual stresses and makes easier to achieve dimensional stability. Thus, it is easier to produce a structure that is stronger and tougher than comparable structures produced by conventional heat treatments due to the fact that the phase transformation is uniform and the structure contains bainite.

## CHAPTER 3

### BAINITE IN STEELS

#### 3.1 Definition

Bainitic steels had been under study thoroughly until it was first discovered by E. S. Davenport and E. C. Bain in 1930. Numerous early researches showed that, this microstructure consists of an ‘acicular, dark etching aggregate’ which is quite unlike pearlite or martensite. [5]

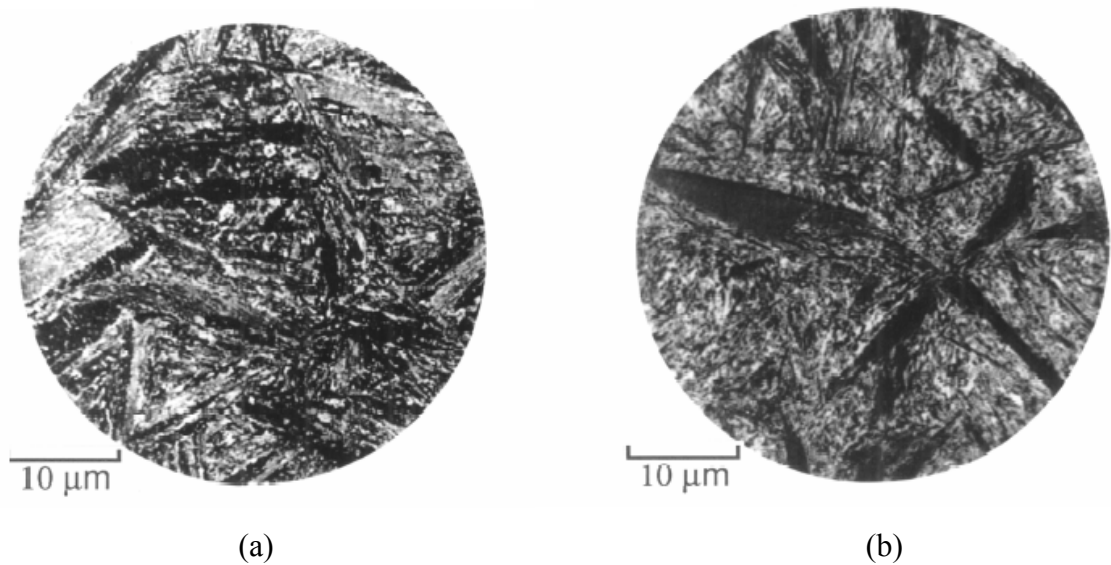


**Figure 3.1** a) Bainite obtained by isothermal transformation at 290 °C

b) Bainite obtained by isothermal transformation at 180 °C

(The micrographs were taken by Vilella and were published in the book *The Alloying Elements in Steel* (Bain, 1939) (Ref. 5)

Earlier researches revealed that, this newly discovered structure – bainite - exhibits unusual and promising properties such as higher toughness for the same hardness than tempered martensite. [1]

Named after Edgar C. Bain, bainite is a microstructure that is formed when austenite is cooled rapidly enough to avoid forming pearlite but cooling is delayed long enough to prevent the formation of martensite. Bainite seems to have some characteristics of both. It is diffusion dependent but does not form the lamellar structures of pearlite. However, like martensite, its structure can be in the form of lath or plate, suggesting shear as well as diffusion. Bainite has some of the hardness properties of martensite and some of the toughness properties of pearlite.

### **3.2 Reaction Mechanism**

A Time-Temperature-Transformation diagram consists of curves representing the transformation times and temperatures of various phases (Fig 3.2). Commercial TTT diagrams usually display overlapped C-curves of different phases when the reactions are fast. However, when reactions are slow, we can separate those curves into two which have different regimes of transformation. The first C-curve, namely the reconstructive transformation, during which the atoms break bonds and diffuse to rearrange themselves which in turn requires mass flow. The second C-curve, on the other hand, requires no diffusion and the transformation happens with the deformation of the parent crystal into the product crystal. In this transformation regime, there is not enough atomic mobility for reconstructive transformation and what's more, the driving force is not sufficient for martensitic transformation, so the product of this mechanism is namely, the bainite.

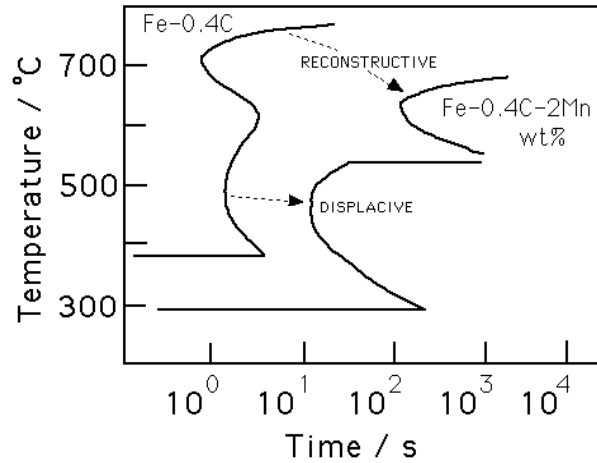


**Figure 3.2** Hypothetical TTT diagram (Ref. 5)

The figure below (Fig. 3.3) shows the atomic point of view of displacive and reconstructive transformations. In the displacive regime, there exists an atomic correspondence accompanied by a physical deformation which causes shape change dominated by strain. On the other hand, reconstructive regime displays rearrangement of atoms without changing the external shape which cannot happen without diffusion. In this regime, atoms partition wherever they are more stable.

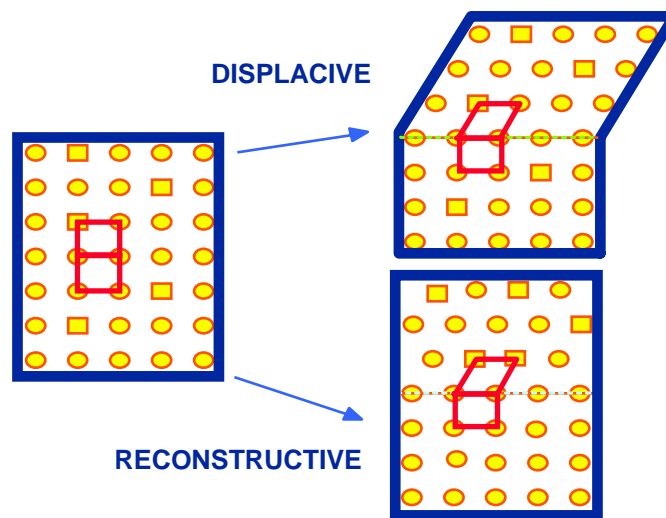


**Figure 3.3** Atomic comparison of displacive and reconstructive transformation (Ref. 5)

### 3.3 Upper and Lower Bainite

The microstructural classification of bainite as “upper” and “lower” is an extremely well established characterization. This classification is basically based on the morphology of the structures that results by different transformation characteristics because of the different temperatures at which the structures form.

Basically upper bainite forms at higher temperatures, whereas lower bainite forms at relatively lower temperatures. This difference results in clear differences in mechanical properties of upper and lower bainite. [5]

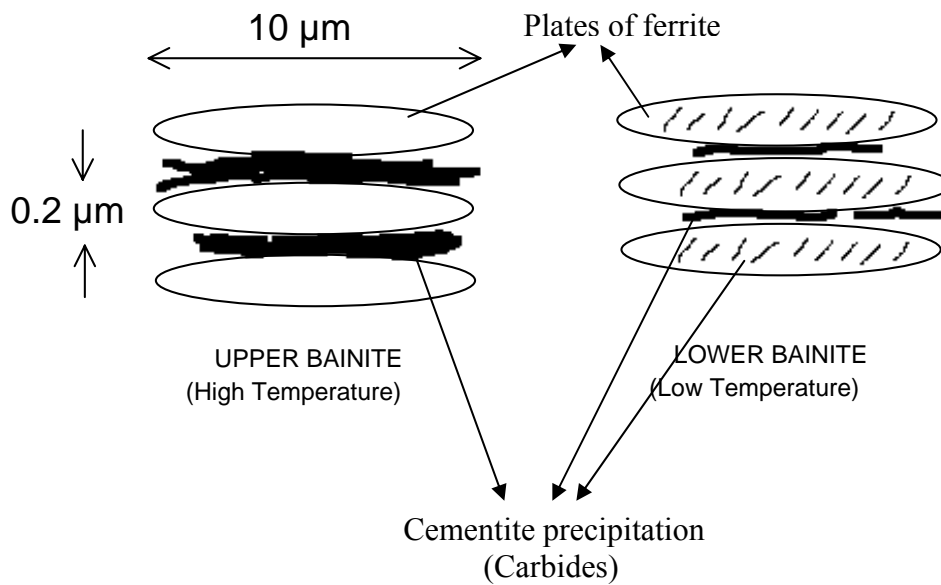


**Figure 3.4** Upper and Lower Bainite

As in Fig. 3.4, the microstructure of both upper and lower bainite is composed of aggregates of small plates or laths of ferrite [5]. The other constituent of the structure is precipitates of cementite (carbide).

The main microstructural difference between upper and lower bainite is the carbide precipitation. In upper bainite, since the transformation temperature is high, the process is fast, thus C atoms do not have sufficient time to precipitate inside ferrite plates (laths). On the other hand, during lower bainite formation, the reaction is slow due to relatively lower temperature, and thus, there is an opportunity for C atoms to precipitate inside the plates.

One important thing here is the ferrite plate size. As in Fig. 3.4, plate size is shown as approximately 10  $\mu\text{m}$ . The bainite mechanism allows a ferrite plate growth to this approximate limited size. After the plate reaches 10  $\mu\text{m}$ , growth stops and a new plate nucleates although there is no obstacle or any other thing that can stop growth. The reason of this phenomenon can be understood by analyzing the following high resolution atomic force microscope plot [5].

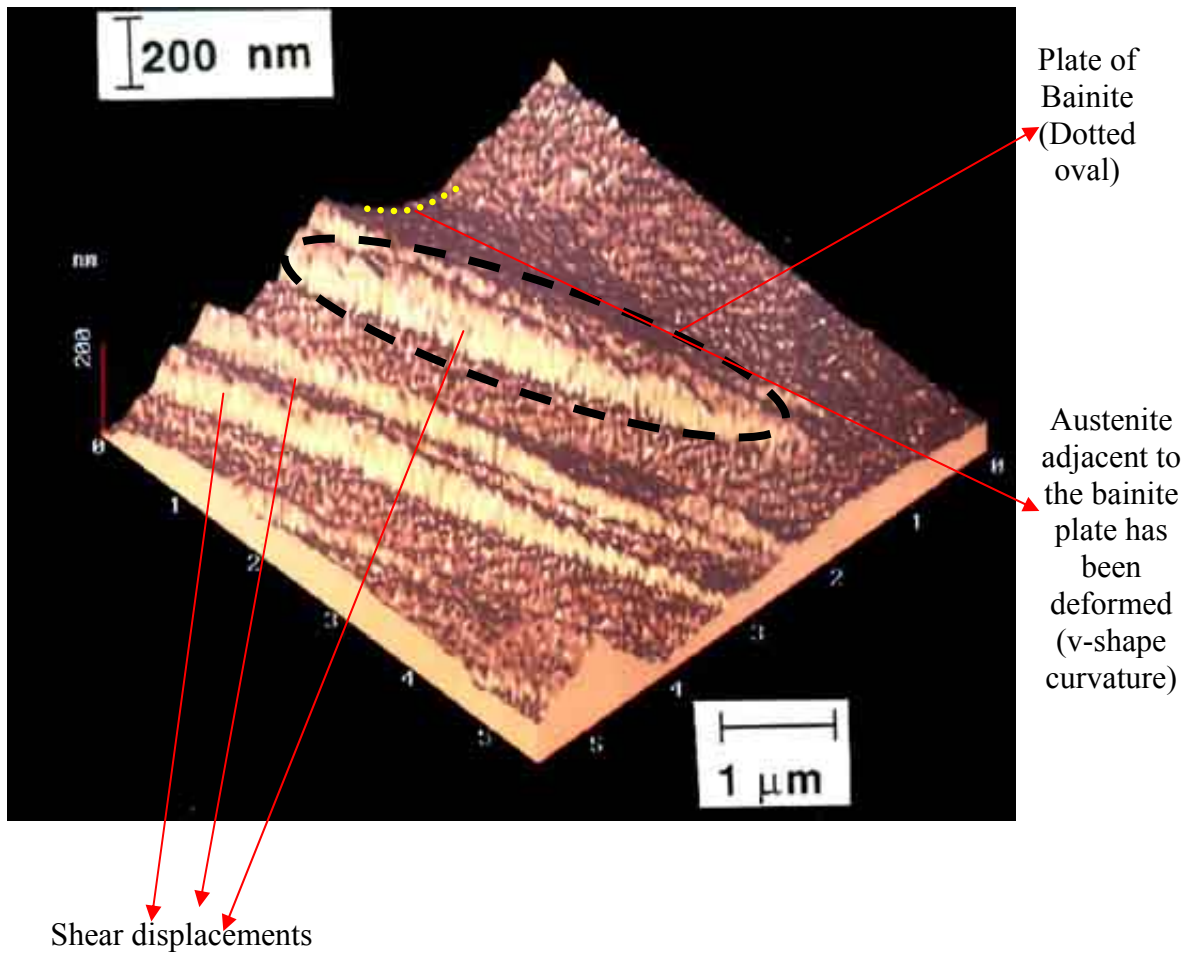


**Figure 3.5** High resolution atomic-force microscope plot. (Ref. 5)

As one of the characteristics of the aforesaid displacive transformation regime of bainite, there exist shear displacements that can be seen on the microscope plot (Fig. 3.5). As can be seen on the figure, the plate of bainite is adjacent to the deformed austenite. The austenite is deformed because it is not strong at that high temperature, and thus it can not accommodate that huge shear strain which in turn causes relaxation of bainite by plastic deformation. So, the v-shape curvature on the plot is packed with dislocations which stop the bainite plate to grow, which in turn causes another plate to nucleate. That is the reason why bainite plates grow only to a limited size. This characteristic makes bainite to have very good mechanical properties since it has a refined microstructure.

As to sum up; bainitic transformation mechanism is displacive and bainite grows without diffusion. However, shortly after growth, Carbon then escapes into the remaining austenite. The shape deformation is plastically accommodated.

### **3.4 Mechanical Properties**

Due to difficulties in obtaining fully bainitic structures in sizable samples of steel, evaluation of the influence of bainite on mechanical properties is difficult.

A steel with composition 0.1% C, 0.0033% B, 0.52% Mn, 0.54% Mo, 0.11% Si composition was found to yield fully bainitic microstructures with very little martensite during normalizing [5]. However, many studies regarding the mechanical properties of bainite revealed that the structures studied were not fully bainitic.

#### **3.4.1 Impact Toughness**

Although the Charpy impact test is empirical and data obtained cannot directly be used in engineering design, it is a vital quality control measure which is used widely in ranking of samples in research and development studies.

An exceptional study was made by Irvine and Pickering [6] by using a normalized low-carbon bainitic steel (0.1 wt% C, 0.003 wt % B, 0.5 wt % Mn, 0.5 wt % Mo) in order to observe the Charpy impact properties. Both upper and lower bainitic structures, heat treated at different temperatures were tested.

It was observed that the impact properties of soft upper bainite tempered at 651 °C for 1 hour were not affected by tempering. Since the microstructure was formed by

transforming at higher temperatures, during which tempering occurs, imposed tempering revealed minor effects on the microstructure.

When tempering was applied at lower temperatures, the stronger upper bainite formed was observed to be more sensitive to tempering.

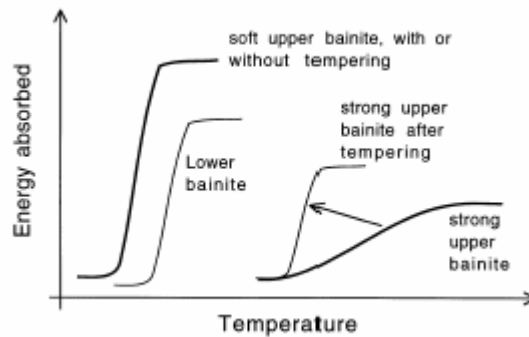


**Figure 3.6** Schematic illustration of impact transition curves (Ref.5)

Irvine and Pickering's study also showed that, lower bainite displayed higher strength and toughness as compared to low strength upper bainite. Much finer carbide particles in lower bainite were responsible for that. What's more, cementite is brittle and cracks under the influence of the stresses generate dislocation pile-ups. Thus, increased dislocation density and more carbides in lower bainitic structures prevent the propagation of cracks. Those factors make cracks intersect carbides or force them to propagate around them which are the reasons for the higher toughness of lower bainite when compared with upper bainite.

Consequently, the results of Irvine and Pickering proved that the most appropriate method of improving the impact properties is to refine the prior austenite grain size, which can be performed by using low transformation temperatures or more properly obtaining lower bainitic structure.

### 3.4.2 Fracture Toughness

A fracture mechanics approach is more reliable than impact testing because a toughness value is obtained, which is a material property, essentially independent of specimen geometry effects [5]. The results of the pre-cracked samples' fracture tests can be used quantitatively to predict whether a structure is likely to fail catastrophically under the influence of the design stress.

In considering the role of bainite or martensite in fracture, it is necessary to note that the phenomenon controlling fracture is the propagation of particle-sized microcracks into the surrounding ferrite matrix, which is called the 'small particle regime'.

In order to relate  $K_{IC}$  values to microstructural and micromechanistic parameters, it must be associated with corresponding critical values of stress  $\sigma_c$  and distance  $r_c$  [7-10]:

$$K_{IC} = \sigma_c(2\pi r_c)^{\frac{1}{2}} \quad (3.1)$$

where  $\sigma_c$  is usually identified with the local stress required to propagate a microcrack nucleus which varies with carbide thickness, or more generally, with the size of the microcrack nuclei resulting from the fracture of a brittle phase in the steel; it is relatively independent of temperature [5].

The interpretation of  $r_c$  is less straightforward. The specimen used in a fracture toughness test is machined to have a crack starting notch and then it is fatigue loaded to form a sharp crack which grows slowly from the root of the notch. The fatigue crack tip is sharp, but not as sharp as the tip of a cleavage crack. It does not therefore propagate when the specimen is tensile loaded for the  $K_{IC}$  test. Instead, the stress field extending from the fatigue crack tip causes brittle particles within a distance  $r_c$  of the tip to fracture. The resulting microcrack nuclei are automatically sharp and propagate into the matrix if

the stress  $\sigma_c$  is exceeded. The cleavage cracks then link up with the original fatigue crack and failure occurs rapidly across the specimen section [5].

Research showed that if the carbide particle size and spatial distribution is bimodal, due perhaps to the presence of a mixture of microstructures, then the  $K_{IC}$  values obtained are likely to show much scatter. Bowen *et al.* [11] found that  $K_{IC}$  values determined for mixed structures of upper and lower bainite (the former containing coarser cementite) exhibited a large degree of scatter when compared with a microstructure of just upper bainite or just martensite.

Bowen *et al.* [11] studied the toughness of tempered martensite and bainite in a low-alloy steel. Their work revealed that  $K_{IC}$  values increased with the test temperature over the range  $-196.5 - 27$  °C (77-300 K). For a given stress, the toughness of bainite was always lower than that of tempered martensite. The fracture stress was in all cases found to be independent of test temperature, but bainite had a lower fracture stress than martensite. These results were explained in terms of measured cementite particle size distributions (Fig. 3.7). The researchers demonstrated that it is not the mean carbide particle size which determines toughness, but the coarsest particles to be found in the microstructure. It has been found that, for a given stress, the toughness increases in the order upper bainite, lower bainite and tempered martensite. On the other hand, it must be mentioned that bainitic structures need not always have poor toughness relative to tempered martensite. All other things being equal, toughness is expected to improve as the strength is reduced, making plastic deformation easy [5].

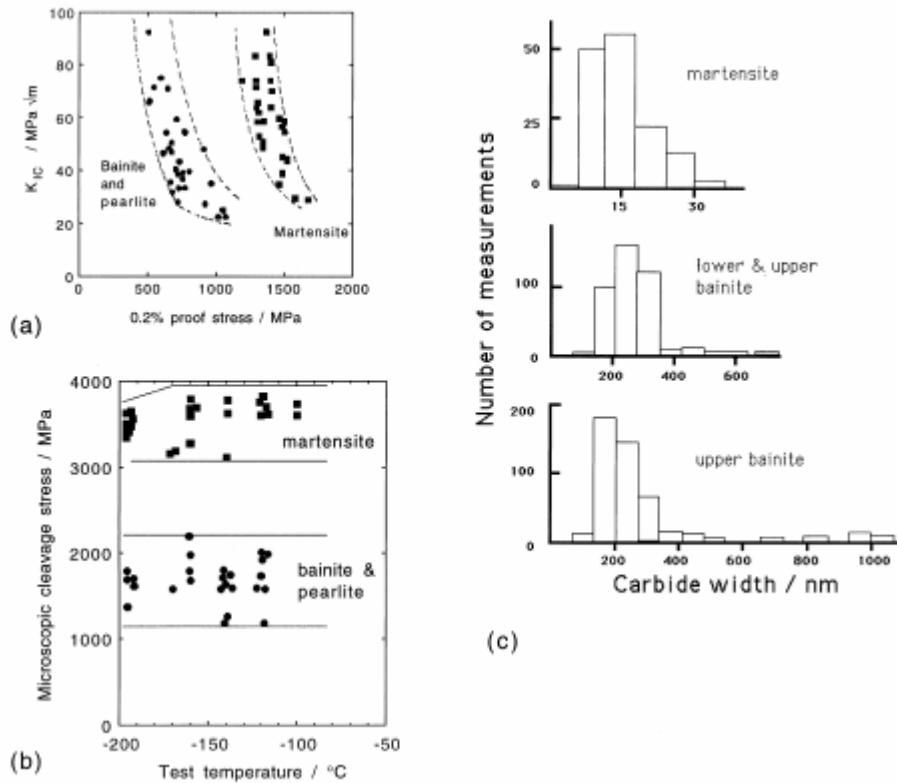


**Figure 3.7** a)  $K_{IC}$  values plotted against corresponding values of the stress b) values plotted against test temperatures c) Carbide size distributions obtained from martensitic and bainitic microstructures (Ref. 5)

Another important point about the before mentioned terms,  $r_c$ , which is the distance over which the stress is large enough to cause carbide cracking is that, it is expected to be small in comparison with the width of a bainite sheaf. According to this, the toughness of bainite or martensite should not be dependent on the austenite grain size or the bainite packet size [5]. This prediction has been demonstrated to be the case for tempered martensite (Bowen *et al.*) but contradictory results exist for bainite. Parker, R. F. [12] and Cao, W. D. *et al.* [13] have reported that small austenite grain size has contribution to toughness. However, this requires appreciable additions of alloying elements for bainitic microstructure to maintain hardenability or special heat treatments.

Another study from Naylor and Krahe [14] by using notched-bar impact tests have shown that a refinement in the bainite packet size leads to an improvement in toughness.

### 3.4.2.1 Cleavage Fracture Path

There exists microstructural evidence that during cleavage failure, the cracks propagate undeviated across individual packets of bainite [15]. Even though adjacent packets of bainite are different crystallographic variants of the orientation relationship, there is a high probability that their cleavage planes are fairly parallel [16]. Fig. 3.8 shows crack propagation in fully bainitic structures.

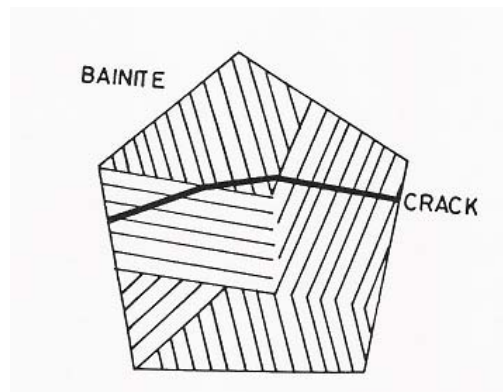


**Figure 3.8** Schematic Illustration of Crack Propagation in Fully Bainitic Microstructures  
(Ref. 17)

There are a number of studies [17-20] which agree that the size of the cleavage facets is important in bainitic structures. The study of Naylor and Krahe [14] also revealed that the facet size correlates well with the width of the bainite packets. They also have shown that the prior austenite grains are partitioned by two types of boundaries: low-void, semicoherent and high-void incoherent boundaries (Fig 3.9)

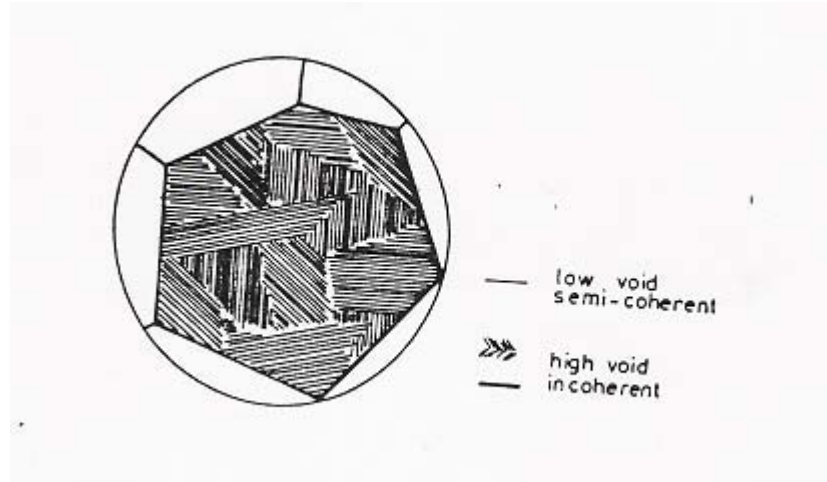


**Figure 3.9** Packets that form in prior austenite grain (Ref. 14)

Regions surrounded by those types of boundaries have been named as packet or subpacket. Direction of a cleavage crack is changed only at the boundary of a packet. Naylor and Krahe concluded that such a direction change causes dissipation of considerable amount of energy at the boundaries. As a result, the improvement in toughness of these structures is mainly due to separation of austenite grain into several pieces by bainitic laths.

Tomita and Okabayashi's research [18] proved that the packet diameter is the primary microstructural parameter controlling the toughness and yield stress. They showed that the mechanical properties are improved with decreasing width of lath present within the packet. Another study by Tomita [21] concentrated on the effect of morphology of ductile second phase for improving the mechanical properties of high strength, low alloy steels with bainitic-martensitic mixed structures.

For mixed bainitic-martensitic structures, the finer facet size which is due to martensite packets, subdivided by bainitic laths is shown schematically in Fig. 3.10.

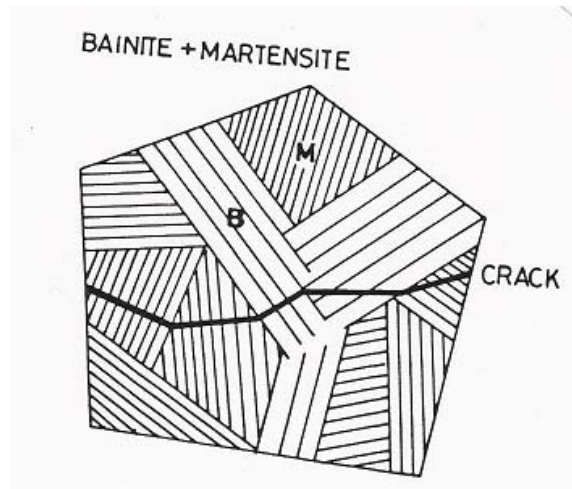


**Figure 3.10** Schematic illustration of crack propagation in bainitic-martensitic mixed microstructures. (Ref. 14)

### 3.4.3 Hardness

For bainitic microstructures, hardness increases linearly with carbon concentration. Irvine and Pickering [22] revealed this linear ratio as about 190 HV per wt%. For martensite, on the other hand, this linear ratio is approximately 950 HV per wt%. Irvine and Pickering have also stated that the austenitizing temperature does not influence the hardness unless it is not high enough to dissolve all the carbides.

For mixed microstructures, the hardness depends on the transformation temperature and composition [5].

In low alloy steels, any untransformed austenite during the bainite reaction may transform into some form of degenerate pearlite. These secondary transformations have an influence on the hardness figures. Lyman and Troiano's work [23] have shown that

for a series of Fe-Cr-C alloys the hardness for the 0.08 wt% C alloy was insensitive to the isothermal transformation temperature (Fig. 3.11).

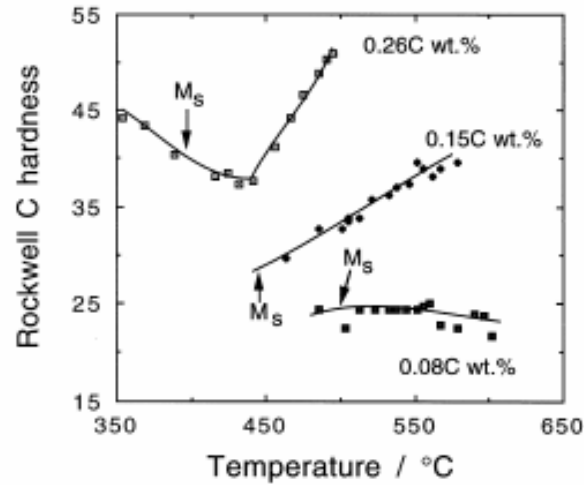


**Figure 3.11** Variation in hardness as a function of the isothermal transformation temperature (Ref. 23)

In their study; the low carbon concentration ensures that the microstructure is almost fully bainitic for all of the temperatures studied. For higher carbon alloys, however, the situation is different as hardness first decreases as the transformation temperature is reduced which is due to the increase in the amount of bainite at the expense of residual phases like martensite and degenerate pearlite.

Kamada *et al.* [24] stated that the hardness of bainite is insensitive to the austenite grain size, even though the grain size influences the bainite sheaf thickness. This situation is expected since the bainite sub-unit size is hardly influenced by the austenite grain size. For the same reason, the hardness of fully bainitic microstructures is not sensitive to the austenitizing temperature [22, 24]

## CHAPTER 4

### LITERATURE REVIEW

A thorough literature search showed that detailed research has been conducted regarding austempering and its effects on mechanical properties of steels.

Liu and Kao [25] studied the toughness and strength combination of low alloy high-strength austempered steels. They have shown that bainite shows extensive strength and toughness properties which are due to refinement of prior austenite grain by lower bainitic martensitic sub-structure. Sandvik and Nevalainen's [26] work proved the same.

Baozhu and Krauss [27] have made valuable research on high temperature mechanical properties of AISI 4340 steels which were isothermally transformed between 200 °C and 430 °C. Their study revealed the differences in energy absorption of lower and upper bainite. Results have shown that tempered martensite and lower bainite absorbed more than twice the energy absorbed by upper bainitic structures. Thus; hardness tests revealed that as the transformation temperature increases, hardness decreases.

Tomita and Okabayashi [28] have also worked on ultra-high strength steel corresponding to AISI 4340. The heat treatment, which they called "The New Heat Treatment", consisted of austenitizing at 860 °C and quenching to a lead tin bath in which isothermal transformation at 320 °C performed. Tempering the steel at 200 °C for 2 hours followed that. The comparison of "The New Heat Treatment" with other conventional methods have shown that, as fraction of lower bainite increases, both yield strength and ultimate strength increases when lower bainite was associated with martensite tempered at 200 °C. This behavior continues and reaches a peak point at 25

vol% bainite. As volume percentage increases beyond that, the strength decreases and reaches to values corresponding to single phase lower bainite.

Another study by Tomita and Okabayashi [29] was associated with AISI 4140 type steel. They applied the same treatment as they did before, and they achieved improved strength, ductility and notch toughness with “The New Heat Treatment”. On the other hand, the new treatment failed at lower temperatures due to absence of Nickel. In the previous study, the expensive alloying element increased the lower temperature intrinsic toughness of the parent martensite when the structure was mixed with martensite and bainite.

Research for higher strength by Tomita and Okibayashi [30] has led them to another heat treatment called “Modified Heat Treatment” (MHT). This new technique consists of “The New Heat Treatment” and multi-austenitization heat treatment in order to increase the strength by keeping the notch toughness at the same level. The microstructure obtained with the MHT consists of 15 vol. % lower bainite with mixed areas of ultra fine grained martensite. In terms of microstructure, MHT displays different structures as compared to “The New Heat Treatment” which had 25 vol. % lower bainite mixed with refined lath martensite. The notch toughness results revealed almost the same values with that of previous work, so, it has been said that the presence of lower bainite is responsible for the improvement of the notch toughness.

Another study has been made by Narosimha et. al. [31]. They used Vanadium containing AISI 4330 type steel. Their study revealed that the presence of upper bainite in a mixed structure leads to a significant improvement in toughness without affecting the strength of the fully martensitic structure. The authors observed no beneficial effect of lower bainite on the mechanical properties and they said this might be due to differences in size and morphology of upper and lower bainites in the mixed structures in AISI 4330 steel.

Researchers have also studied the effects of different alloying elements, especially Nickel. Tomita [32] was one of them who worked on the effect of different levels of Ni

and Cr on toughness and strength of three high-C low-alloy steel. The study consists of austempering just above the  $M_s$  which in turn produced mixed structure of lower bainite and martensite providing the best combination of toughness and strength. The best mechanical properties were observed within the steel having the highest Ni (1.8%) content. The author suggested that Ni changes the intrinsic toughness of the parent martensite by facilitating the cross-slip during deformation, thus increases the mechanical properties.

Another study about the effects of Ni was made by Joarder and Sarma [33]. They have observed the effect of austempering 3.6% Ni steel at different temperatures. The results revealed that Ni has a strong stabilizing effect on retained austenite films at the lath boundaries of martensite. The applied heat treatment formed both upper and lower bainite at 450 °C, while completely lower bainite was observed below 400 °C.

The effect of austempering on a different steel was studied by Kurtulus [34] by using DIN 34CrNiMo5 gun barrel steel. Austempering was applied at four different temperatures in the range of 300 °C – 375 °C with 25 °C increments. Different austempering time periods were also investigated at constant austempering temperatures. Microstructural and mechanical analysis revealed that there is an inverse relationship between the austempering temperature and impact toughness of the steel studied.

Although much of the austempering studies done in the recent years concentrate on ductile iron, considerable studies regarding steels with various alloying elements have been made by Li and Wu [35]. The low carbon alloy steel they used showed enhanced mechanical properties due to strain-induced martensite transformation and transformation-induced plasticity (TRIP) of retained austenite when it was strained at temperatures between  $M_s$  and  $M_d$ , since retained austenite was moderately stabilized due to carbon enrichment by austempering. The methodology they used is associated with different austempering temperatures and reaching maximum values for tensile strength, total elongation and strength-ductility balance.

One of the most recent studies of austempering treatment for steels have been made by Mirak and Nili-Ahmadabadi [36]. In their study, an AISI 4130 type steel was used and isothermal, successive and up-quenching heat treatments were used to improve the mechanical properties. They studied mechanical properties by testing sub-sized tensile and Charpy impact specimens. The results showed that successive austempering improves the mechanical properties compared with continuous cooling and conventional austempering. However, it was shown that the best combination of mechanical properties is achieved when an up-quenching heat treatment is used. Their microstructural studies showed that partition of grains by lower bainite is probably the main reason for this improvement.

Another austempering study regarding high carbon steel have been made by Putatunda [37]. He examined the influence of austempering temperature on the microstructure and mechanical properties of a high-carbon (1.00%), high-silicon (3.00%) and high-manganese (2.00%) cast steel. The study consists of four different austempering treatments. Mechanical properties were studied by conducting tensile and fracture toughness tests. Test results indicated that maximum fracture toughness was obtained when the microstructure contains very high austenitic carbon (X-gamma C-gamma).

Putatunda has also studied the influence of austempering on the microstructure and mechanical properties of an alloyed cast steel containing high silicon (3.00%) and high manganese (2.00%) [38]. The mechanical aspect of the study was the influence of microstructure on the plain strain fracture toughness. The test results were rather regarded the amount of austenite within the structure and showed that by using a suitable austempering process, i.e. by austenitizing at 1010 °C for 2 hr and then subsequently austempering at 316 °C for 6 hr, it is possible to produce more than 80% austenite in the matrix of the material. The mechanical tests showed that austempering resulted in a significant improvement in mechanical properties as well as fracture toughness of the material.

The effect of austempering on mechanical properties of a high silicon steel was studied by Li and Chen [39]. With the conducted experiments, an ausferrite structure consisting of bainitic ferrite and retained austenite was obtained by austempering the high silicon cast steel in a large temperature range (240 °C - 400 °C). Another outcome of the study was that; a full ausferrite structure could be obtained by austempering the steel with a silicon content around 2.64%. Lower silicon would result in the formation of martensite, and excessive silicon would cause pro-eutectoid ferrite in the structure. The results showed that the full ausferrite structure has high strength, toughness and hardness. With increasing silicon content, the strength decreases, the hardness keeps unchanged and the toughness first increases to a maximum value and then decreases.

Another recent study about austempering by Putatunda is about fracture toughness of a high carbon and high silicon steel [40]. The study consists of the influence of austempering temperature on the microstructure and the mechanical properties (fracture toughness) of this steel at room temperature and in ambient atmosphere. Test specimens were austenitized at 927 °C for 2 hours and then austempered at several temperatures between 260 °C and 399 °C for a fixed time period of 2 hours to produce different microstructures. The test results showed that the maximum fracture toughness is obtained in this steel with an upper bainitic microstructure when the microstructure contains about 35% austenite and the carbon content in the austenite is about 2%. The retained austenite and its carbon content increased with austempering temperature, reaching a peak value at 385 °C and then retained austenite decreased with increasing temperature. The carbon content of the austenite also showed a similar behavior. The fracture toughness was found to depend on the parameter  $(X\text{-}\gamma \text{ C-}\gamma/d)^{1/2}$  where X- $\gamma$  is the volume fraction of the austenite, C- $\gamma$  is the carbon content of austenite and d is the mean free path of dislocation motion in ferrite.

On the other hand, Lee's work [41] is concerned with a correlation of plane strain fracture toughness and microstructure in two steels corresponding to AISI 4340 composition. Steels used in the study were vacuum induction melted and then deoxidized with aluminum and titanium-aluminum additions, respectively. In the case of

the aluminum killed steel, austenitizing at temperatures above 950 °C led to large austenite grain sizes, whereas in the titanium steel, grain sizes were maintained below about 70  $\mu$ m even after austenitizing at temperatures up to 1200 °C. This allowed a comparison of variations in plane strain fracture toughness with austenitizing temperature. The results indicated that the spacing of finer particles, e.g. carbides not dissolved in the austenitizing process, is of primary importance in controlling fracture toughness. In quenched and tempered microstructures, fracture toughness was found to scale monotonically with plane strain tensile ductility and particle spacing. However, the simple correlations between toughness and ductility broke down in microstructures produced by step quenching or double austenitizing.

## CHAPTER 5

### EXPERIMENTAL PROCEDURE

The material used in this experimental study is 35NiCrMoV12.5. Specimens are provided from MKE Heavy Weapon and Steel Factory located in Kirikkale in the shape of semi-circular parts with a circular hollow shape at the center as shown in Fig. 5.1 and Fig. 5.2. A set of pre-machined, single edge notch bend (SENB) specimens were also provided by the same place.

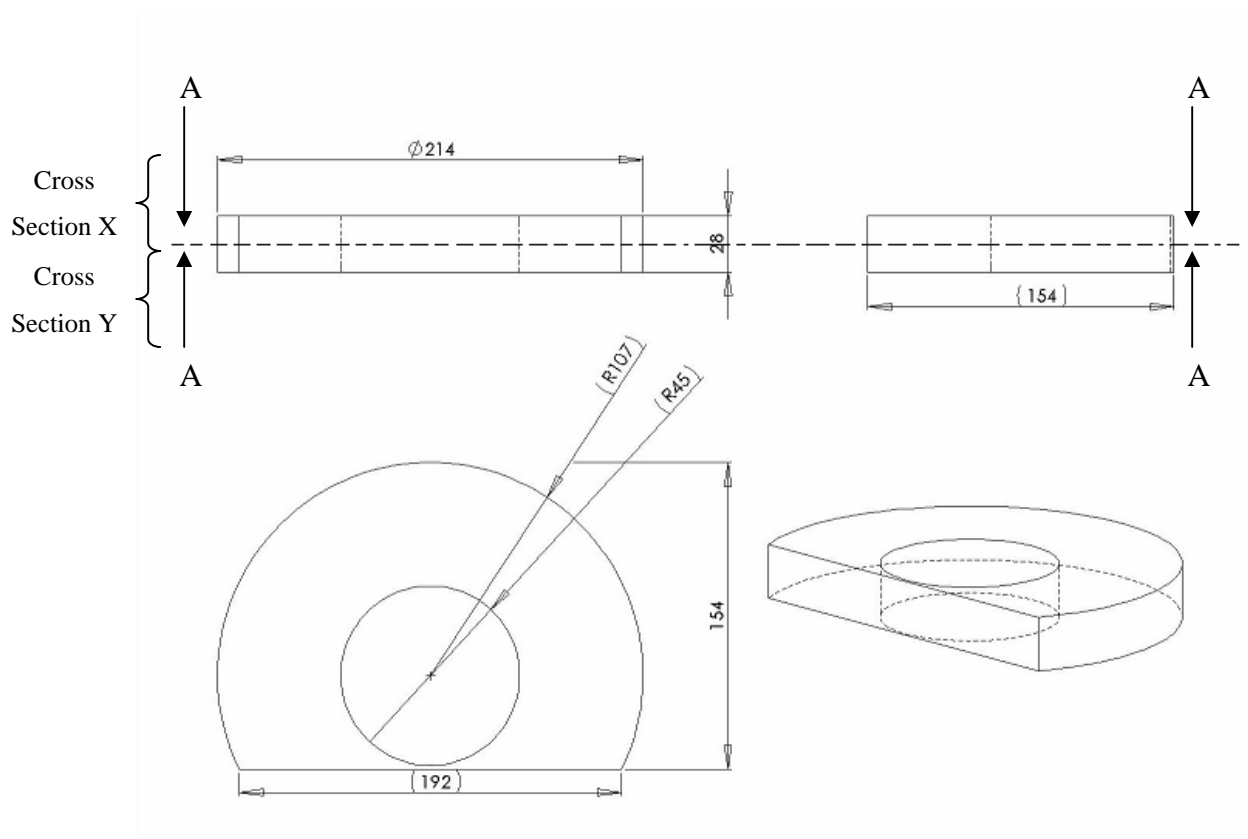


**Figure 5.1** Specimen shape and dimensions (all in mm)

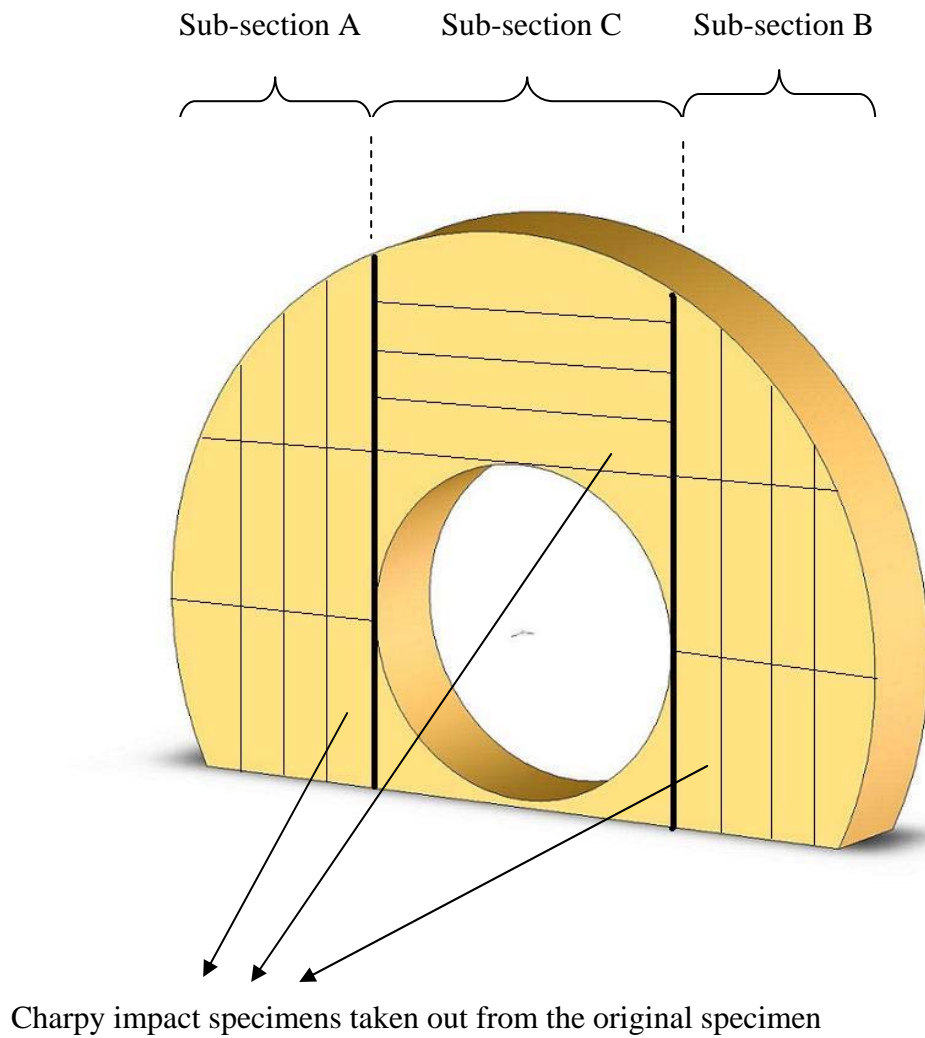


**Figure 5.2** Schematic illustration of the coding scheme and Charpy samples extracted from the original specimen

## 5.1 Chemical Composition

Two different semi-circular specimens are obtained from the factory with specimen numbers 20 and 30. The other specimens are in the shape of SENB bars. The compositional analyses of all the samples are as follows:

**Table 5.1** Chemical composition of the specimens used

<b><u>Specimen no</u></b>	<b><u>Material</u></b>	<b><u>%C</u></b>	<b><u>%Mn</u></b>	<b><u>%Si</u></b>	<b><u>%P</u></b>	<b><u>%S</u></b>	<b><u>%Cr</u></b>	<b><u>%Ni</u></b>	<b><u>%Mo</u></b>	<b><u>%V</u></b>
20	35NiCrMoV12.5	0.38	0.47	0.33	0.007	0.004	1.29	2.97	0.43	0.09
30	35NiCrMoV12.5	0.35	0.43	0.27	0.006	0.006	1.29	2.93	0.43	0.09
SENB	35NiCrMoV12.5	0.38	0.41	0.28	0.002	0.003	1.31	3.06	0.43	0.10

## 5.2 Sampling of Specimens 20 & 30

Regarding the shape of the obtained semi-circular specimens, a coding and numbering scheme is developed in order to take the radial mechanical differences into account and to distinguish which mechanical test specimens come from which position.

First, the part is cut into two identical cross- sections (Cross-sections X and Y, Fig 4.1) through A-A direction. Then the obtained cross sections are cut into 11\*11\*51 mm pieces through the lines shown in Fig. 5.2. The ASTM standard dimensions for charpy v-notch test specimen are 10\*10\*50 mm. However, due to probable unwanted surface effects that might occur during heat treatment, the specimens were first cut into slightly larger specimens which were in turn grinded into exact ASTM dimensions.

Due to the production technique applied, the mechanical properties that are examined in this study might display differences according to the location where the specimen is

taken from the original specimen. Therefore, the original specimen is divided into three sub-sections which are coded A, B and C as in Fig. 5.2. Next, the charpy test specimens from these sections are numbered respectively also by taking the cross-section (either X or Y) which they come from into account.

The following illustration explains the coding technique applied:

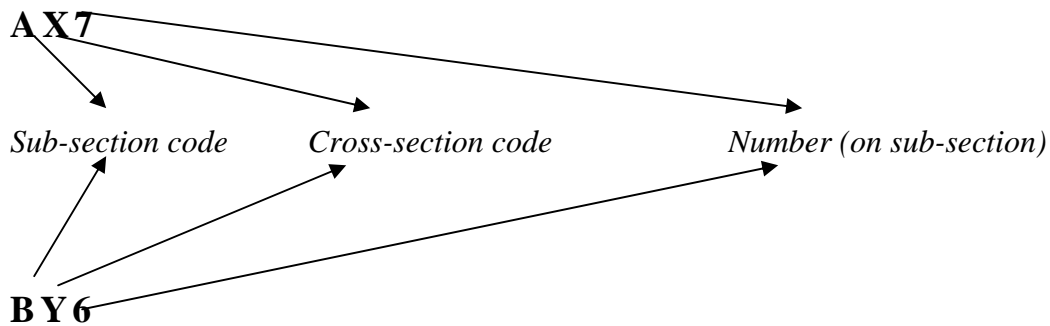


**Figure 5.3** Illustration of the coding technique

### **5.3 Heat Treatment Pre-study**

Due to the fact that the chemical composition of AISI 4340 steel is similar to that of 35NiCrMoV12.5's, TTT diagram of 4340 steel is used as a reference during this study. Fig. 5.4 shows the TTT diagram for AISI 4340.

A brief, though thorough check was made to see if AISI 4340 steel is suitable for austempering procedure as it is described in Metals Handbook [2]. As can be seen on the diagram, first; the location of the nose of the TTT curve allows significant time to bypass it. Second, the time required for complete transformation of austenite to bainite at the chosen austempering temperatures is suitable for such an experimental work. And finally, the location of the  $M_s$  point (approximately 275 °C) allows the aforesaid laboratory work.

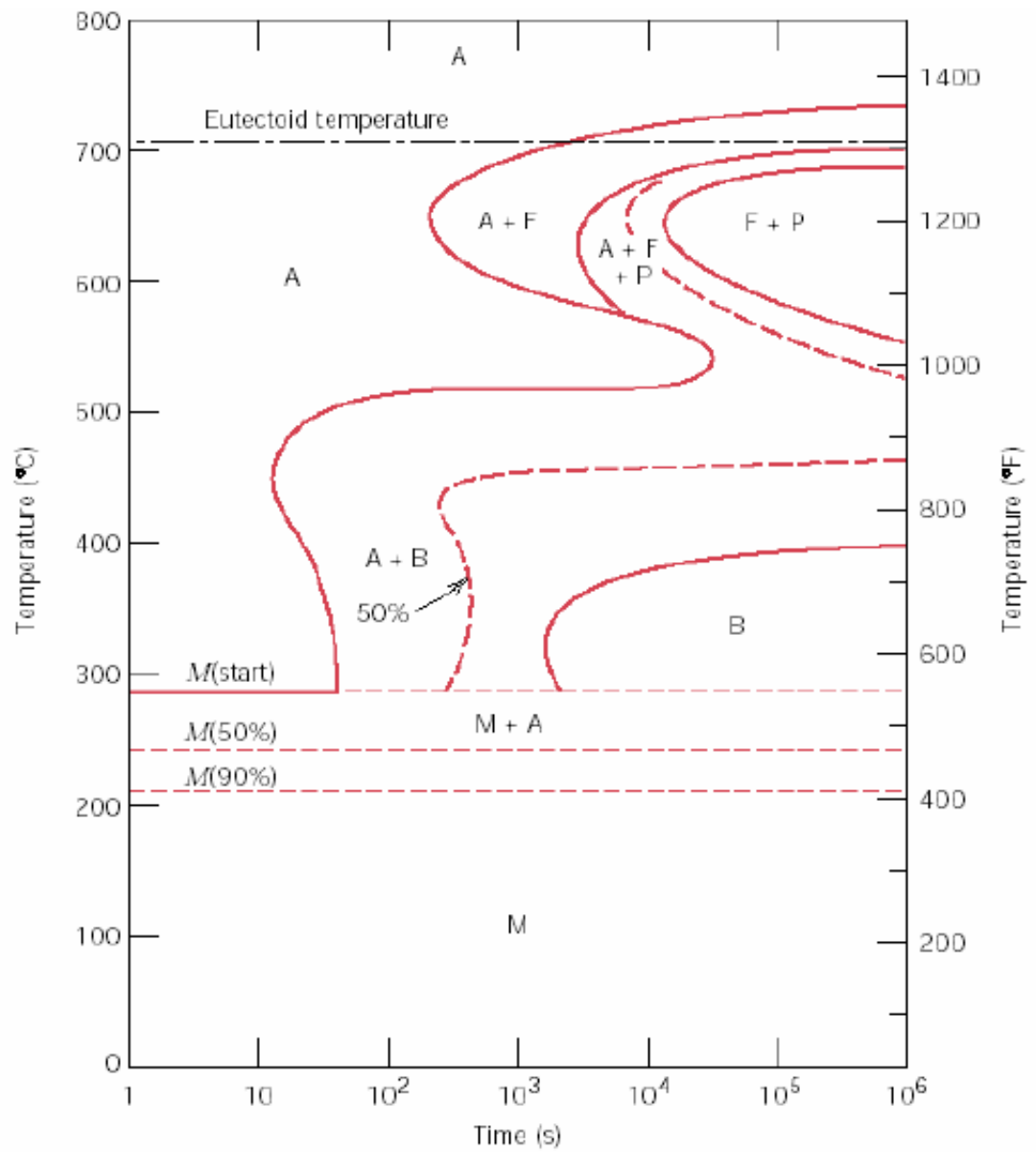


**Figure 5.4** AISI 4340 Time-Temperature-Transformation Diagram

Another check, whether using the AISI 4340's TTT diagram as a reference is appropriate to be used in this study, is the  $M_s$  temperature control. The following empirical formula by Nehrenberg [42] is used to estimate the  $M_s$  temperature. The result is as follows:

$$M_s = 500 - (300 * \%C) - (33 * \%Mn) - (22 * \%Cr) - (17 * \%Ni) - (11 * \%Si) - (11 * \%Mo) \quad (\text{in } ^\circ\text{C}) \quad (5.1)$$

Since there are 2 different original specimens used in this study, 2 different  $M_s$  temperatures exist. In order to get an estimate, two  $M_s$  temperatures are calculated and averaged.

For specimens 20 and 30, the calculated  $M_s$  temperatures are 283 °C and 294 °C respectively. So the average calculated  $M_s$  temperature with the above formula is 289 °C.

Another formula used in  $M_s$  temperature estimation is as follows: [43]

$$M_s = 1000 - (650 * \%C) - (70 * \%Mn) - (70 * \%Cr) - (35 * \%Ni) - (50 * \%Mo) \quad (\text{in } ^\circ\text{F}) \quad (5.2)$$

By applying the same procedure, the calculated  $M_s$  temperatures are as follows: 262 °C for specimen 20, and 275 °C for specimen 30. The average temperature is 269 °C, which is pretty close to  $M_s$  temperature of AISI 4340 (~ 275 °C).

Another empirical formula used for the same purpose is as follows: [1]

$$M_s = 538 - (361 * \%C) - (39 * \%Mn) - (19 * \%Ni) - (39 * \%Cr) \quad (\text{in } ^\circ\text{C}) \quad (5.3)$$

Calculated  $M_s$  temperatures with the above formula gives the following results: 275 °C for specimen 20, and 288 °C for specimen 30. The average temperature is 282 °C, which again is very close to AISI 4340's  $M_s$ .

As a result; all these reveal that, AISI 4340 TTT diagram is a good reference for this study.

#### 5.4 Heat Treatment Procedure

As a result of a thorough literature study and careful interpretation of the AISI 4340 steel's TTT diagram, three austempering temperatures and four time intervals are selected. The following scheme is applied to un-notched Charpy bar and pre-machined SENB samples. The austenitizing temperature and time are 850 °C and 1 hour. Austempering is applied within a salt bath heated to the desired temperature. Quenching media is water.

**Table 5.2** Austempering temperatures and times investigated in the study

<b>Charpy specimen</b>	350 °C	1 min	10 min	1 hr	10 hr
<b>Charpy specimen</b>	325 °C	1 min	10 min	1 hr	10 hr
<b>Charpy specimen</b>	300 °C	1 min	10 min	1 hr	10 hr
<b>SENB specimen</b>	325 °C	5 hr	-	-	-

An illustration of the austempering procedure applied is shown in the figure below (Fig. 5.5).

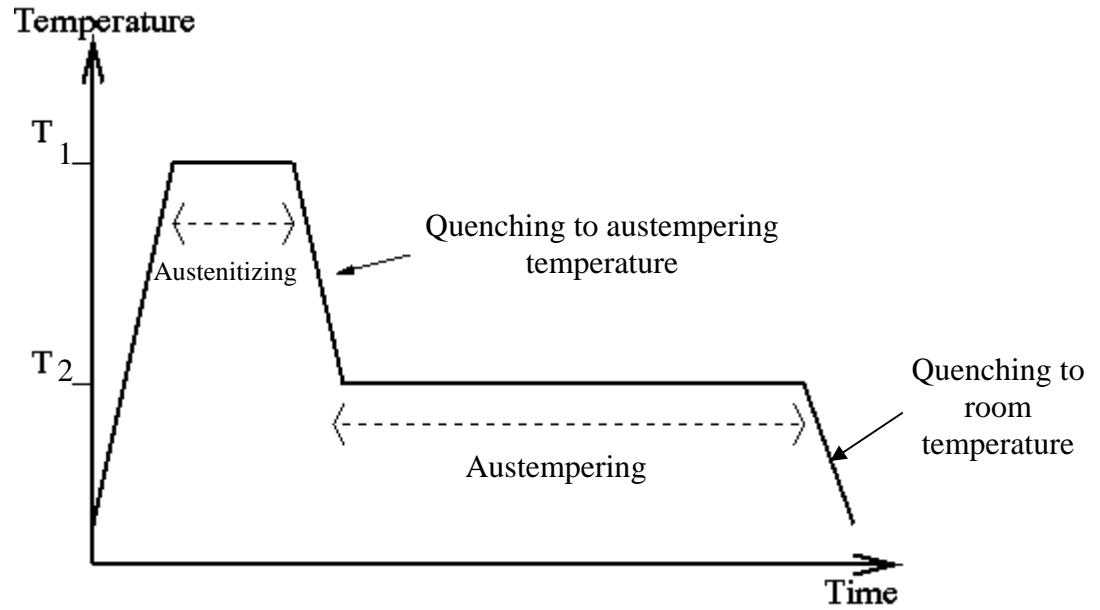


**Figure 5.5** Austempering procedure applied

Protherm laboratory type furnace with a maximum temperature of 1150 °C is used for austenitizing and tempering. The experimental setup is shown in figure 5.6.



**Figure 5.6** The experimental setup.

After applying the austempering heat treatment, another preliminary study was made in order to find an appropriate tempering temperature with the aim of making a comparison between the mechanical properties obtained after austempering and conventional quenching and tempering methods.

1\*1\*1 mm cubes are cut and conventional quenching and tempering applied at the following temperatures for 40 minutes: 300 °C, 350 °C, 400 °C, 450 °C, 500 °C. Hardness values of the samples measured and compared with that of obtained after austempering. The following hardness (Rockwell C) values are obtained.

**Table 5.3** Conventional quenching and tempering temperatures and corresponding hardness values

<b>Tempering Temperature (°C)</b>	<b>Hardness (Rockwell C)</b>
500	38
450	42
400	44
350	46
300	48
Austenitized and quenched	52

After comparing the results of the tempering study with that of austempering, 400 °C is chosen to apply as the tempering temperature both to charpy and SENB specimens. Tempering time is 2 hours for SENB, 40 minutes for charpy samples.

## 5.5 Notched Bar Impact Test (Charpy)

The standard ASTM procedure defined with designation number E 23 - 93a (Standard Test Methods for Notched Bar Impact Testing of Metallic Materials) is applied in this study. The test consists of measuring the energy absorbed in breaking, by one blow from a pendulum. A test piece notched in the middle and supported at one end can be seen in figures 5.7 and 5.8.

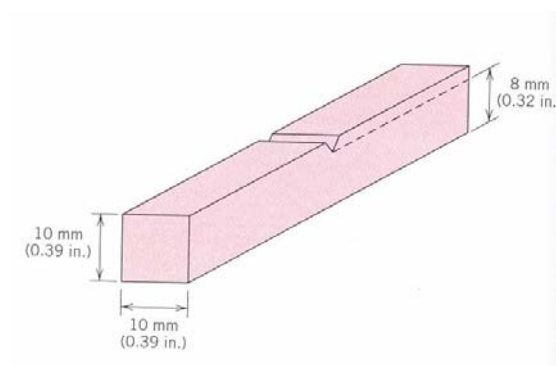


**Figure 5.7** The standard charpy test specimen

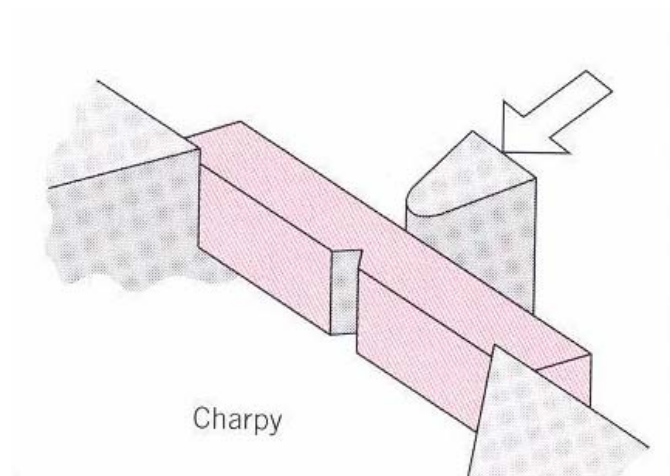


**Figure 5.8** Illustration of the charpy impact test and the direction of the force applied



**Figure 5.9** Charpy impact bar samples prepared after heat treatment

A Tinius & Olsen Charpy impact test machine was used in the experiment.



**Figure 5.10** Charpy impact test machine used.

## 5.6 Hardness Test

The standard ASTM procedure defined with designation number E 18 – 1989 is applied by using a digital Emco M4U-025 Rockwell Hardness Tester in C scale under a major load of 150 kgf.



**Figure 5.11** Hardness test machine

## 5.7 Fracture Toughness Test

The standard ASTM procedure defined with designation number E 399 – 90 (Standard Test Method for Plane-Strain Fracture Toughness of Metallic Materials) is applied in this study. Figure 5.12 shows the standard single edge notch bend (SENB) specimen.

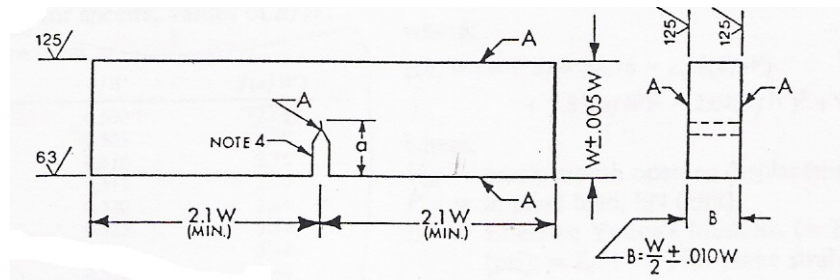


**Figure 5.12** Standard SENB test specimen

MTS 810 Materials Test System is used for fatigue crack initiation. Also Laboratory Equipment is used for fracturing the specimens until failure.



**Figure 5.13** MTS Testing machine in operation during pre-cracking the specimens



**Figure 5.14** Alsa Laboratory Machine used to fracture the specimens until failure

## 5.8 Optical Microscopy

Nikon Optiphot-100 optical microscope with a digital camera attached to it was used to analyze the microstructures obtained at the end of heat treatments.



**Figure 5.15** Optical microscope used

## 5.9 Electron Microscopy

A JEOL, JSM-6400 electron microscope, equipped with NORAN System 6 X-ray Microanalysis System & Semafore Digitizer was used for detailed analyses of the microstructures obtained.

## CHAPTER 6

### RESULTS

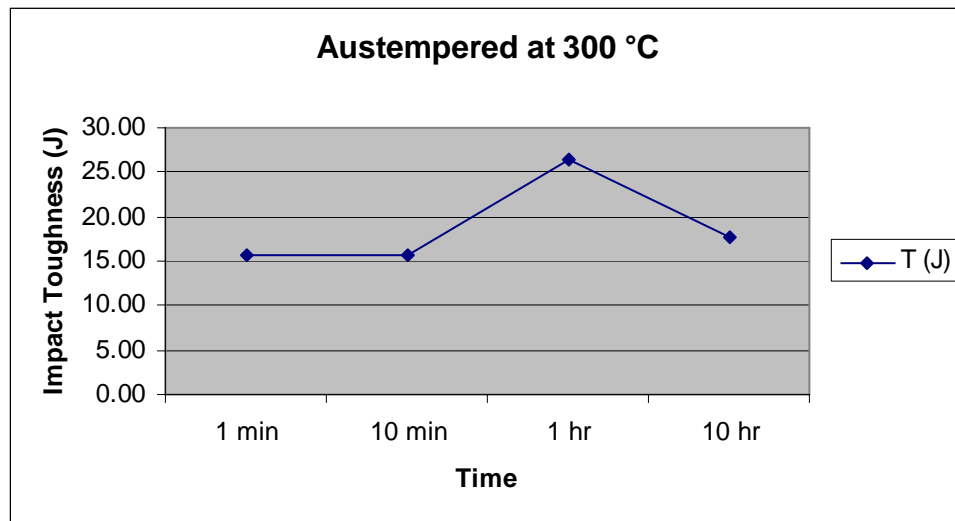
#### 6.1 Charpy Impact Test

The results of the Charpy tests applied to austempered samples are shown in Table 6.1. Three test specimens were tested and the averages of the three figures are listed in the table.

**Table 6.1** Charpy impact test results of the austempered specimens.

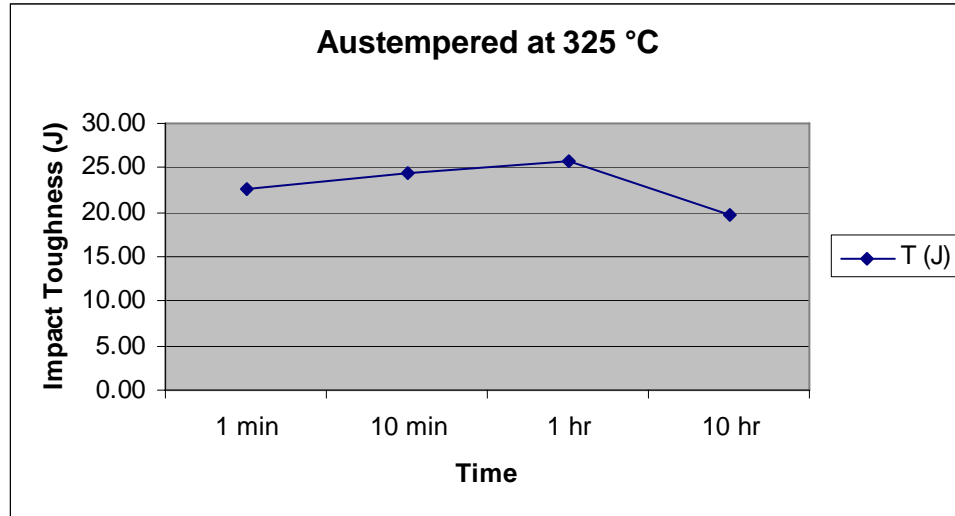
<b>Austempering Temperature (°C)</b>	<b>Austempering time</b>	<b>Impact Toughness (J)</b>
<b>300</b>	1 min	16
	10 min	16
	1 hr	27
	10 hr	18
<b>325</b>	1 min	23
	10 min	25
	1 hr	26
	10 hr	20
<b>350</b>	1 min	28
	10 min	23
	1 hr	17
	10 hr	16

Figure 6.1 shows the impact toughness values obtained for the specimens that were austempered at 300 °C. Different austempering times produced different toughness values. Although the values obtained are the same for 1 minute and for 10 minutes, there exists an increase when the parts were transformed for 1 hour. The lower value obtained at 10 hours is not expectable and hard to explain.



**Figure 6.1** Impact Toughness values of the specimens which were austempered at 300 °C.

Parts austempered at 325 °C display a somewhat similar trend to parts transformed at 300°C (Figure 6.2). Once more the highest toughness was obtained at 1 hour and following that there is a decrease in toughness measurements.



**Figure 6.2** Impact Toughness values of the specimens which were austempered at 325 °C.

As opposed to the expected trend, at 350 °C, impact toughness values are observed to decrease with austempering time right from the beginning of the transformation (Fig. 6.3). This situation is hard to explain, since the exact same conditions and procedures were applied to all specimens throughout the study. When the specimens are examined with respect to the places they have taken out from the original part, again, it is not possible to find a logical explanation.

It would be more acceptable if there would exist an initial increase in toughness as it was occurred at 300 °C and 325 °C. However, such a trend did not appear at 350 °C. It is not possible to explain how toughness decreased throughout the transformation, since the amount of bainite should have increased in time, which would make the steel tougher.

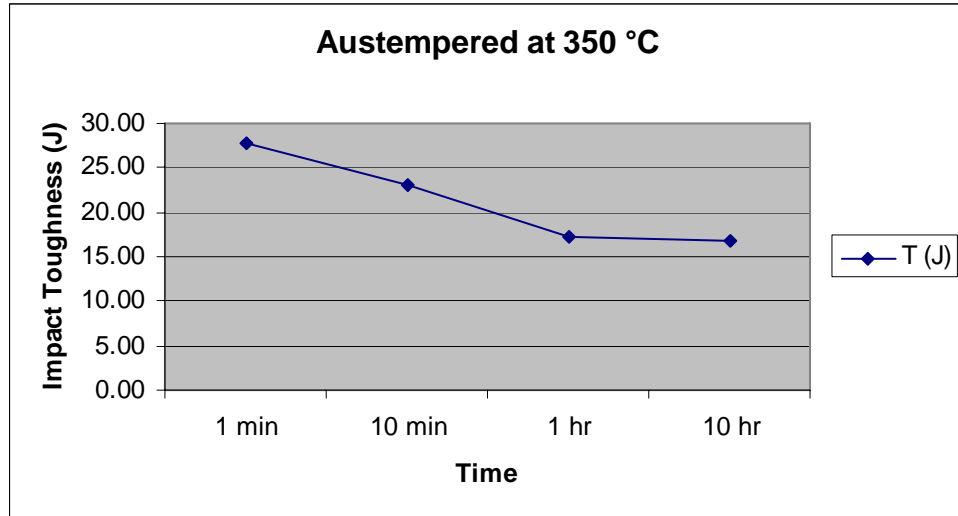


**Figure 6.3** Impact Toughness values of the specimens which were austempered at 350 °C.

## 6.2 Hardness Test

The following table (Table 6.2) shows the values obtained for the hardness test. Three measurements are taken from each sample and the averages are listed in the table.

**Table 6.2** Hardness results of the austempered specimens.

<b>Austempering Temperature (°C)</b>	<b>Austempering time</b>	<b>Hardness (HRC)</b>
<b>300</b>	1 min	55
	10 min	56
	1 hr	48
	10 hr	46
<b>325</b>	1 min	53
	10 min	52
	1 hr	45
	10 hr	44
<b>350</b>	1 min	54
	10 min	52
	1 hr	44
	10 hr	41

As can be seen on figures 6.4, 6.5 and 6.6, hardness decreases with increasing transformation periods. The significant change in the hardness values was occurred again when the transformation time was increased from 10 minutes to 1 hour. The same trend was observed in the impact toughness measurements at 300 °C and 325 °C.

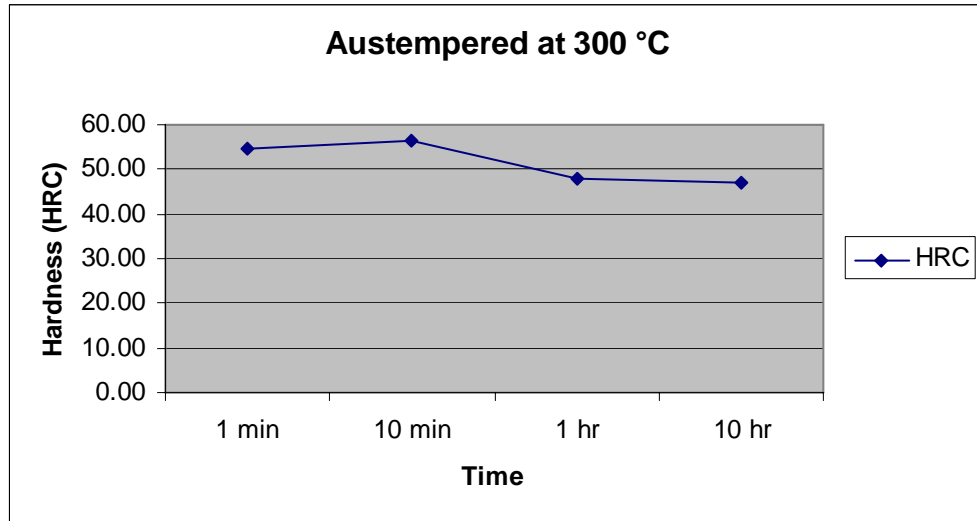


**Figure 6.4** Hardness values of the specimens which were austempered at 300 °C.

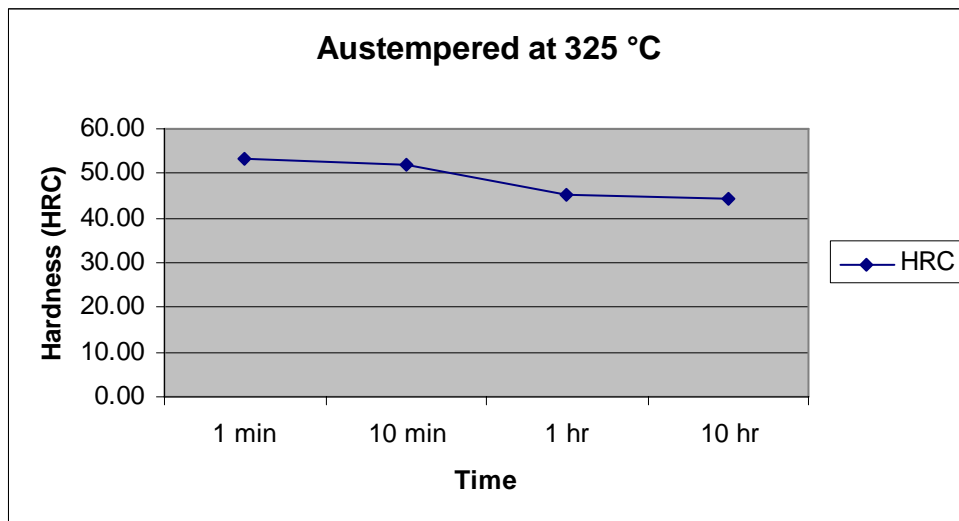


**Figure 6.5** Hardness values of the specimens which were austempered at 325 °C.

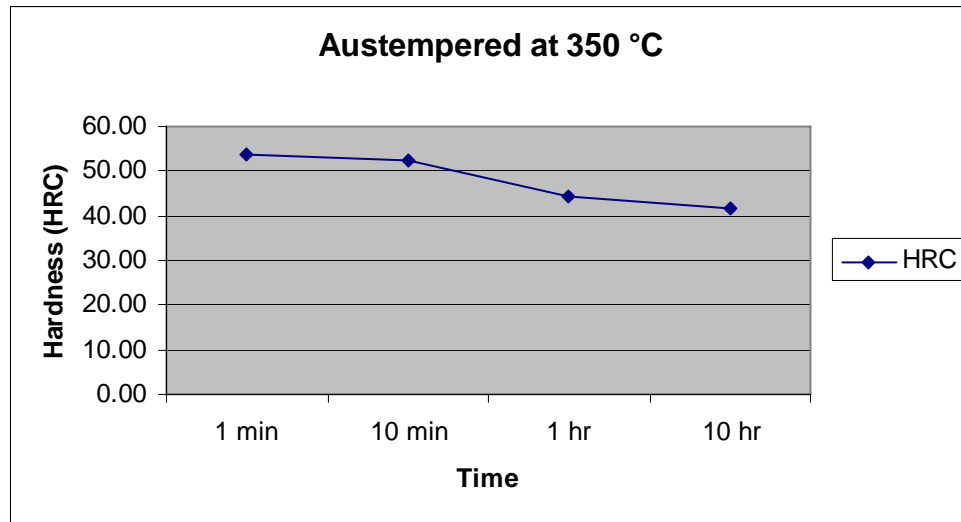


**Figure 6.6** Hardness values of the specimens which were austempered at 350 °C.

### 6.3 Fracture Toughness Test

Tables 6.3 and 6.4 display the  $K_Q$  values obtained for austempered and conventionally quenched and tempered specimens. The austempering temperature is 325 °C and isothermal holding time is 5 hours. On the other hand, tempering was applied at 400 °C, and parts hold isothermally for 2 hours.

In order the following values to be considered as plain-strain fracture toughness ( $K_{IC}$ ) values; they should have passed some validity tests as it is described in the ASTM standard. However, none of the samples tested, except FN 2.3, provided the desired dimensional conditions, so every single value obtained is a  $K_Q$  value higher than  $K_{IC}$ .

As can be seen in tables 6.3 and 6.4, the values obtained are pretty consistent with each other, and there is not much scatter. The interesting result obtained here is that; all the values obtained after austempering are lower than the values obtained after conventional quenching and tempering. Possible reasoning is done in the next chapter.

**Table 6.3** Fracture Toughness Test Results of the Austempered specimens

<b>Specimen Number</b>	<b>B (mm)</b>	<b>W (mm)</b>	<b>a (mm)</b>	<b>a/W</b>	<b>f(a/W)</b>	<b>P<sub>Q</sub> (N)</b>	<b>K<sub>Q</sub> (N.mm<sup>-3/2</sup>)</b>
<b>FN 2.1</b>	17.95	36.01	19.19	0.533	2.99	27949	<b>3091.65</b>
<b>FN 2.3</b>	18	36.1	18.44	0.511	2.75	27851	<b>2815.09</b>
<b>FN 2.6</b>	18	36.05	18.63	0.517	2.79	30401	<b>3124.02</b>

**Table 6.4** Fracture Toughness Test Results of the Conventional Quenched and Tempered specimens.

<b>Specimen Number</b>	<b>B (mm)</b>	<b>W (mm)</b>	<b>a (mm)</b>	<b>a/W</b>	<b>f(a/W)</b>	<b>P<sub>Q</sub> (N)</b>	<b>K<sub>Q</sub> (N.mm<sup>-3/2</sup>)</b>
<b>FN 2.2</b>	17.88	36.05	18.67	0.518	2.84	32656	<b>3438.81</b>
<b>FN 2.4</b>	17.93	36.05	18.37	0.510	2.75	33931	<b>3450.19</b>
<b>FN 2.5</b>	17.8	35.88	18.46	0.514	2.79	32754	<b>3427.85</b>

## CHAPTER 7

### DISCUSSION

#### 7.1 Charpy Impact Test

The impact toughness of the original specimen (as received) is 38 joules. As can be seen on table 6.1, none of the austempered samples could reach that toughness level. As received samples have undergone various other heat treatment procedures (normalization, quenching and tempering) which made the steel tougher than the austempering treatment applied in this study.

Figure 6.1 shows the toughness trend obtained for 300 °C. The same toughness values obtained for 1 minute and 10 minutes transformations is barely understandable. It could be true only under such circumstances in which nucleation is in its very early steps and the structure is predominantly martensite. Only this would make the values obtained reasonable. However, the reference TTT diagram used displays no such appearance.

Examination of the austempering temperatures and the impact toughness values obtained at 300 °C and 325 °C together reveals that, at constant temperature, as austempering time increases, higher impact toughness values are obtained. This behavior can be seen in figures 6.1 and 6.2. However, the increasing trend in toughness values was observed to occur until 1 hour transformation. The next toughness value measured was lower than the value obtained in 1 hour. This scheme was observed both at 300 °C and 325 °C clearly.

The important factor that affects the toughness in austempered structures is the packet size. In martensite and bainite, these packets share the same austenite grain and they

divide austenite grain into several sub-grains where direction of crack is deflected by dissipating considerable amount of energy [20]. The number of packets increases as we increase the holding time at these particular temperatures. As the number of packets increase, the dimensions of the bainitic colonies decrease. Thus, there exist more packets with smaller colonies. As a result, as isothermal holding time increases we obtain more bainite. Bainite has a tougher structure as compared to martensite, which would occur if we quench the part, due to the precipitation of carbides which align with the same angle in the matrix of ferrite. Consequently, it is observed that the toughness of the steel increases as austempering time increases until some point.

What happens after that point is of great interest. It would seem reasonable that the strong carbide forming elements in our steel, such as V, Cr, Mo, might have made austenite to decompose into ferrite and carbides, which in turn decreased the toughness values obtained. However, this reasoning is not valid under the circumstances of this study since the steel used has a carbon concentration of 0.35%-0.38%. Such low amount of carbon makes this reasoning not logical.

If we neglect the decreasing trend at 350 °C and take toughness values individually, a comparison of the austempering temperatures can be seen in figure 7.1. When the highest and lowest temperatures are considered (300 °C and 350 °C), it can be seen that at 1 hour, the highest impact toughness value is obtained at 300 °C and there is a high difference between the values of 300 °C and 350 °C. Likewise, 325 °C treatment reached its maximum toughness at 1 hour which is again higher than the value obtained at 350 °C.

We can conclude that almost all values obtained at 300 °C and 325 °C are higher than that of 350 °C. This situation is consistent with the work of Irvine and Pickering [6] and it is reasonable because lower temperature bainite contains finer carbide particles. What's more, cementite is brittle and cracks under the influence of the stresses generate dislocation pile-ups. Thus, increased dislocation density and more carbides in lower bainitic structures prevent the propagation of cracks. Those factors make cracks intersect

carbides or force them to propagate around them which are the reasons for the higher toughness of lower bainite when compared with upper temperature bainite.

A contradictory result to previous explanation, however, was found during short transformation times. Especially 1 minute holding period reveals that the highest austempering temperature provides the highest toughness. However, normally one would expect to obtain higher impact values as transformation occurs at relatively lower temperatures. The explanation to this result, especially for 1 minute transformation period would be due to the shape of the TTT curve. Since the C shape curves define the regions which different structures form, at 1 minute, the bainite start curve could be in such a shape that the amount of bainite transformed is higher at 350 °C than at 300 °C and 325 °C. Another thing that can be said is that, 1 minute measurements resembled such figures that can be obtained with a treatment that is almost equivalent to martempering.

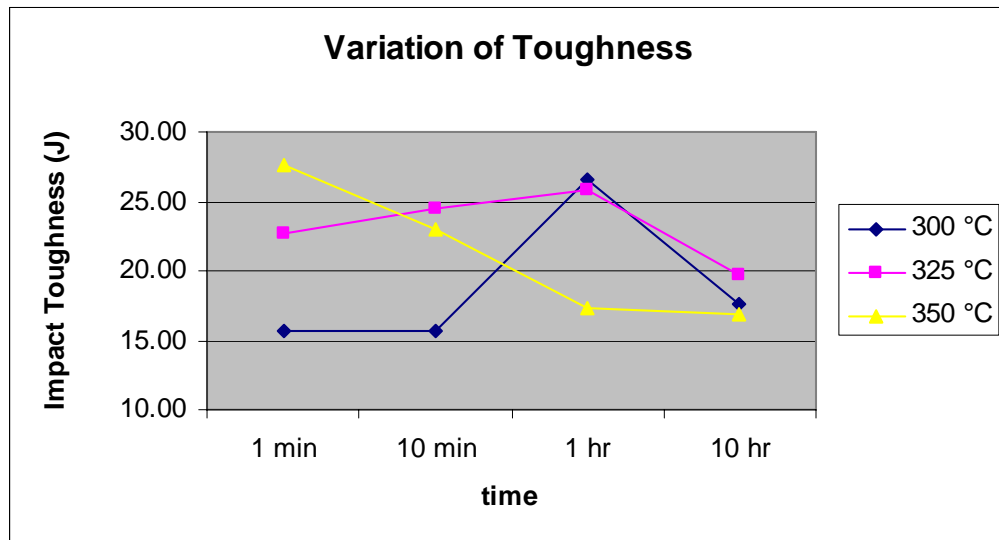


**Figure 7.1** Comparison of different austempering temperatures with respect to impact toughness values obtained at different transformation times. (Y-axis range is 10 J - 30 J)

Figure 7.2 provides a better visualization of different austempering times. The expected behavior is observed with the 1 hour plot (yellow line). At constant time, toughness decreases with temperature. However, 1 minute plot revealed the exact opposite behavior which might be due to the explanation above regarding C shape transformation curves.

The decrease in toughness as temperature increases from 325 °C to 350 °C can be observed for 10 minutes, 1 hour and 10 hours plots (pink, yellow and light blue lines). This is consistent with the common bainitic behavior as discussed above.

The best illustration of the effect of time in toughness can be seen with 325 °C. As isothermal transformation time increases, impact toughness increases. However, this trend is up to 10 hours.

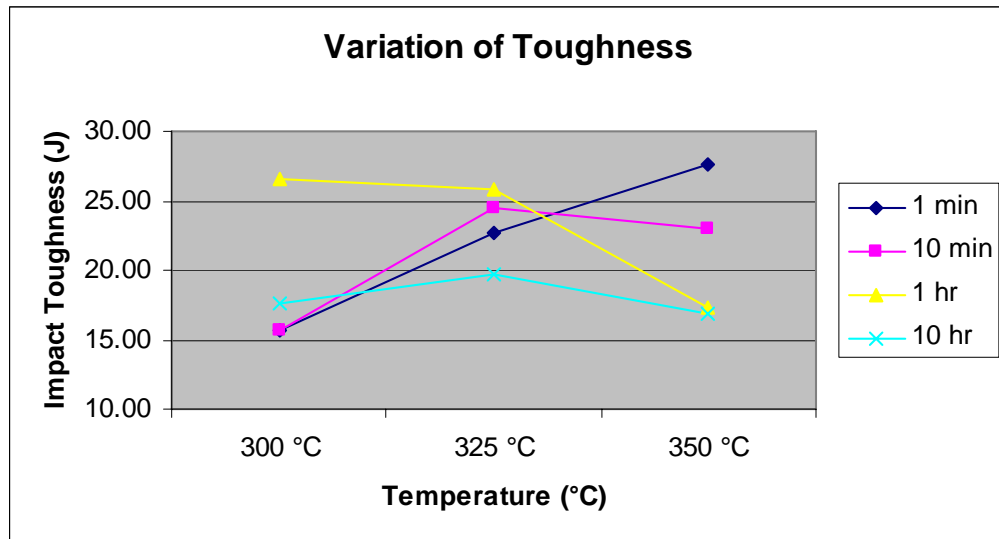


**Figure 7.2** Comparison of different austempering times with respect to impact toughness values obtained at different transformation temperatures.

(Y-axis range is 10 J - 30 J)

A quick comparison of the values obtained by conventional quenching and tempering and by austempering reveals an interesting situation. As it is explained in chapter 5, 400 °C was chosen as the tempering temperature. The approximate average hardness value of 1 hour and 10 hours austempered specimens is 44 HRC. The same hardness value is obtained at 400 °C with the preliminary tempering tests, so 400 °C was used as the tempering temperature.

During conventional quenching and tempering study, impact Charpy specimens were first austenitized at 850 °C and then quenched in water. Next, tempering was applied and parts were tested under exactly the same conditions as before. Conventionally treated specimens displayed an impact toughness value of 40 J. This value is higher than every single value obtained with austempering throughout this study.

An important point to mention here is the machining of the Charpy impact test samples. Due to machining problems faced during the preparation of samples, especially during the notch preparation step, dimensional differences have occurred between test specimens. Standard Charpy samples were not easy to produce all the time. Most probably, this resulted in some deviations in the impact toughness values obtained. Consequently, unpredictable and hard to explain results might be due to this machining problem.

## 7.2 Hardness Test

The hardness of the original specimens (as received) is approximately 39 HRC. As in table 6.2, every hardness value obtained in this study displays a higher level of hardness than the original parts. The existence of the hard and brittle phase martensite is the main reason of the higher hardness values obtained. At all transformation temperatures, hardness values decreased as isothermal holding time increased.

All temperatures have somewhat displayed a similar hardness trend as austempering time increased. This was due to the transformation of austenite to bainite. As isothermal holding time increased, the amount of bainite in the microstructure increased. As the amount of bainite increased, there was less austenite to transform to martensite during quenching following austempering. As a result, there occurred a decreasing trend in hardness as austempering time increases.

When the longest and shortest austempering times are compared, it can be seen that there is a difference of at least 8 HRC when considering 300 °C and 325 °C (Figure 7.3). This difference is almost 12 HRC when considering 350 °C. Similarly, all temperatures display an almost identical trend with respect to austempering time. Especially 325 °C and 350 °C display almost the same hardness values except the longest austempering time.

Fine grain size, high carbide precipitation and high dislocation density are the main factors that make bainite stronger. These factors increase with decreasing austempering temperature. It can be seen that the measurements taken from the 300 °C specimens are slightly higher than the others. This situation is consistent with the accepted models of bainite.

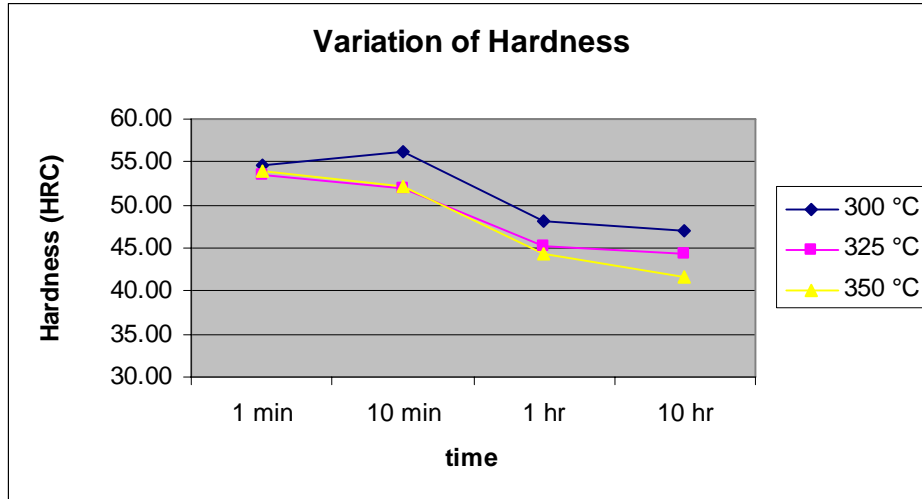


**Figure 7.3** Comparison of the austempering temperatures with respect to hardness values obtained at different transformation times. (Y-axis range is 30 HRC – 60 HRC)

When figure 7.4 is analyzed, it is easier to see that the same austempering times have very similar hardness values at three different temperatures. Once more, it can easily be seen that longer isothermal holding times reveal lower hardness values.

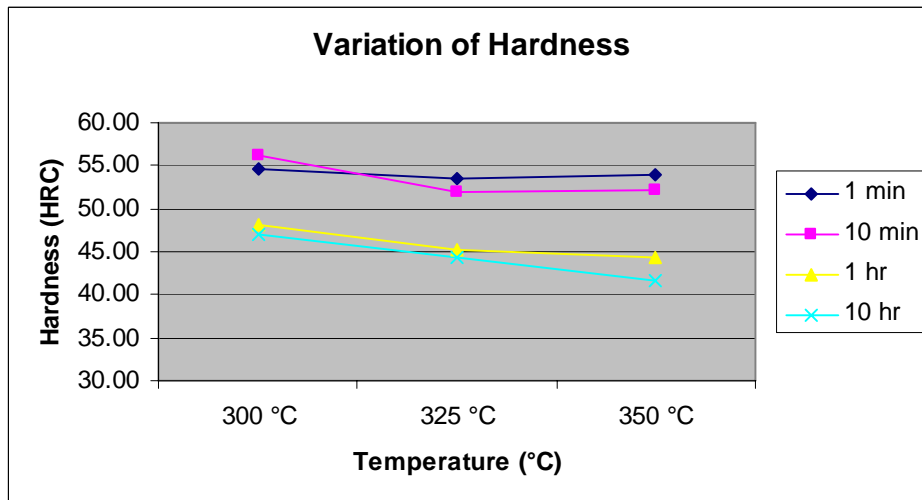


**Figure 7.4** Comparison of the austempering times with respect to hardness values obtained at different transformation temperatures. (Y-axis range is 30 HRC – 60 HRC)

### 7.3 Fracture Toughness Test

When interpreting the fracture toughness values, it is useful to mention that, the phenomenon controlling fracture is the propagation of particle sized microcracks into the surrounding ferrite matrix.

The  $K_Q$  values obtained throughout this study do not show much scatter and especially the values obtained for tempered specimens are highly consistent within each other.

The analysis and comparison of the results of the two different treatments can be seen in figure 7.5.

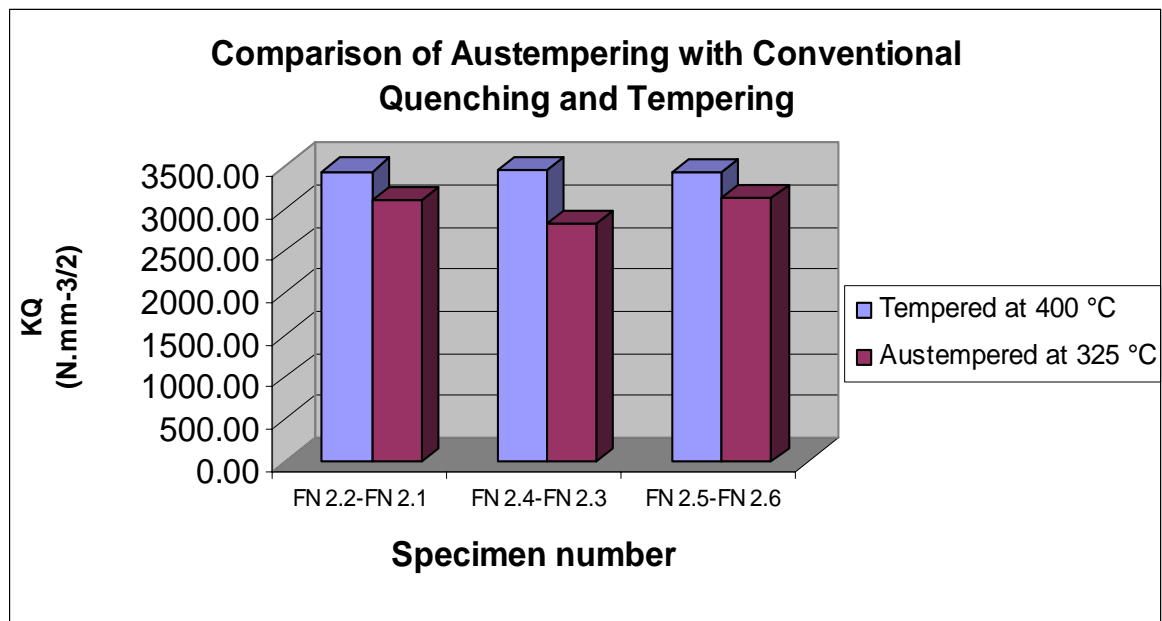


**Figure 7.5** Comparison of the fracture toughness values of austempered and conventionally quenched and tempered specimens.

As can be seen easily in figure 7.5, conventional quenching and tempering provided better fracture toughness values. Although it is expected to receive higher toughness values from the tougher phase bainite, the result obtained is consistent with that of Bowen *et al.* [11]. Although the fracture testing temperature they used was not room temperature, as it is in our case, they found that for a given stress, the toughness of bainite was always lower than that of tempered martensite. They stated that the fracture stress is independent of the test temperature, and bainite has a lower fracture stress than tempered martensite.

Although it was not possible to conduct such a study throughout this work, Bowen *et al.* explained this situation in terms of measured cementite particle size distributions.

The researchers demonstrated that it is not the mean carbide particle size which determines toughness, but the coarsest particles to be found in the microstructure. It has been found that, for a given stress, the toughness increases in the order upper bainite, lower bainite and tempered martensite.

On the other hand, it must be mentioned that bainitic structures do not always have poor toughness relative to tempered martensite. Liu and Kao [25] and Sandvik and Nevalainen [26] have shown that, due to refinement of prior austenite grain by lower bainitic martensitic sub-structure, bainite shows extensive toughness.

One of the important factors that probably have affected the toughness of the austempered specimens is the size of the austempering salt bath used. With respect to specimen size, bath used could have been slightly larger which would have eliminated any doubts about the possibility of quick increases in bath temperature. Another option could be using smaller compact tension test specimens which would be more appropriate when the bath size is considered. However, it was not possible due to specimen supply in hand.

## 7.4 Microstructural Features

The microstructural interpretations of the above mechanical studies are investigated by means of optical and electron microscopy. Higher magnifications with optical microscopy such as 2400 was enough most of the time. However, colonies and sheaves of microstructures are much easier to observe with scanning electron microscopy. Further study of the samples with transmission electron microscopy is necessary in some conditions which could not be done in this study.

As it is stated by Chang and Bhadeshia [48], lower bainitic structures can contain a strongly bimodal size distribution of plates. A number of studies [49-51] have also mentioned that it is easier to observe a few coarse plates on an optical scale; however the remaining microstructure consists of much finer plates which can only be resolved using transmission electron microscopy.

Although it is easier to observe fine platelets of lower bainite that nucleate at austenite grain boundaries during isothermal transformation at relatively higher temperatures, lower temperatures (large undercooling) make the structure coalesce into coarser plates [48].

Large undercooling below the bainite start temperature is mainly the case in this study. A FORTRAN program [52] was used to calculate the  $B_s$  temperature. The calculated value was approximately 400 °C, which is also consistent with the TTT diagram used. As a result, the temperatures tested in this study, especially the lower ones, tend to reveal coarser bainitic plates.

In ferrous alloys, equilibrium microstructures such as pearlite, ferrite or cementite have a general morphology and easily recognized on many occasions. However, bainite and martensite have a different situation. They may appear in many different morphologies according to cooling rate and to the chemical composition of the initial sample [53].

When examined on a fine scale, different microstructures can be obtained when the same heat treatment is applied to steels with different chemical compositions. For example, bainite is generally recognized by its finger-like ferrite sheaves, but the length and morphology of these sheaves or the location and direction of the carbides that form within bainite may differ. This difference arises due to local differences in chemical composition, isothermal transformation temperature and its relative position on the TTT diagram [53].

Due to aforesaid reasons and difficulty of distinguishing between bainite and martensite, reference 100% martensite samples were prepared for comparison purposes. Figure 7.6 shows fully martensitic microstructures.

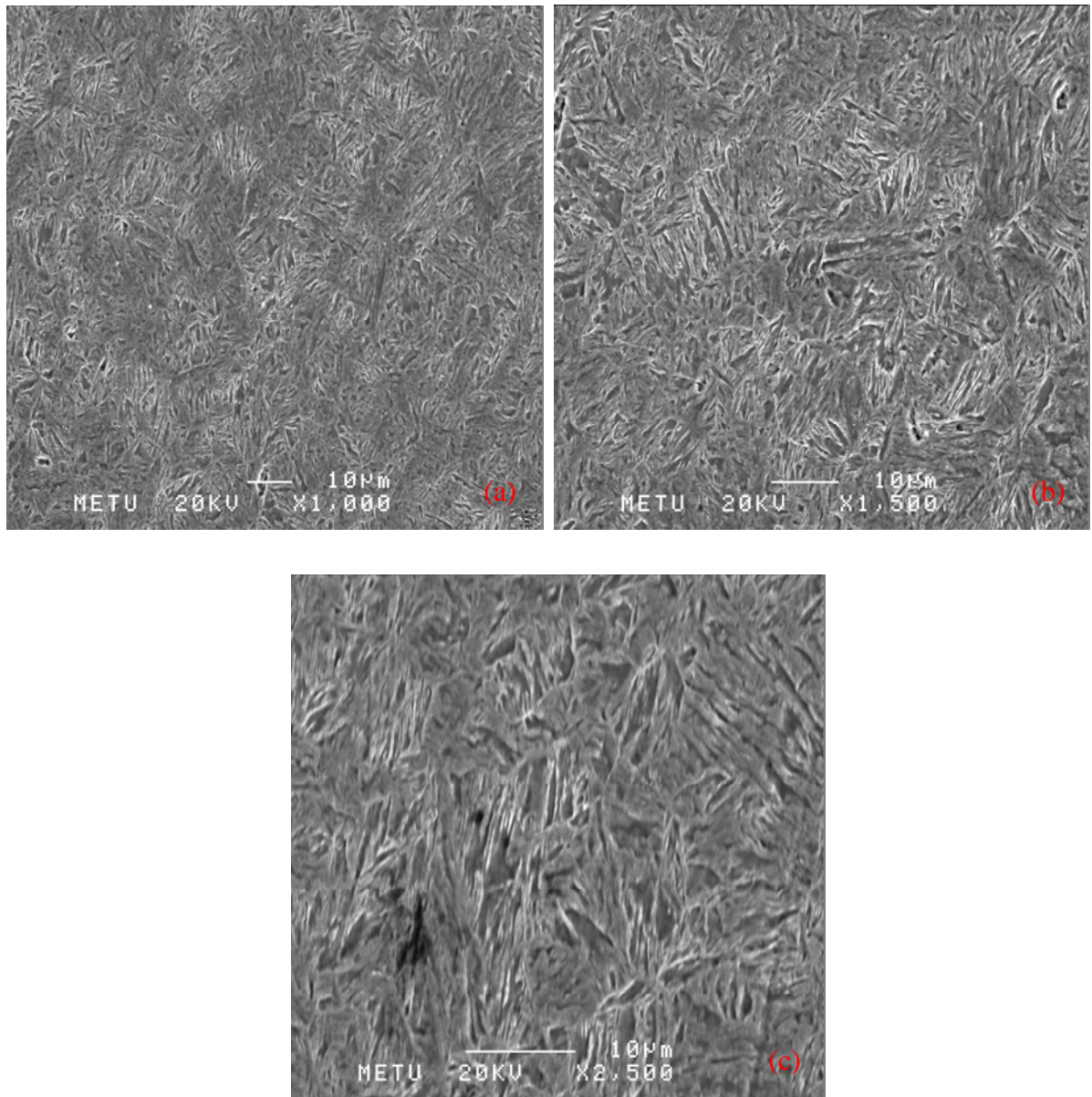
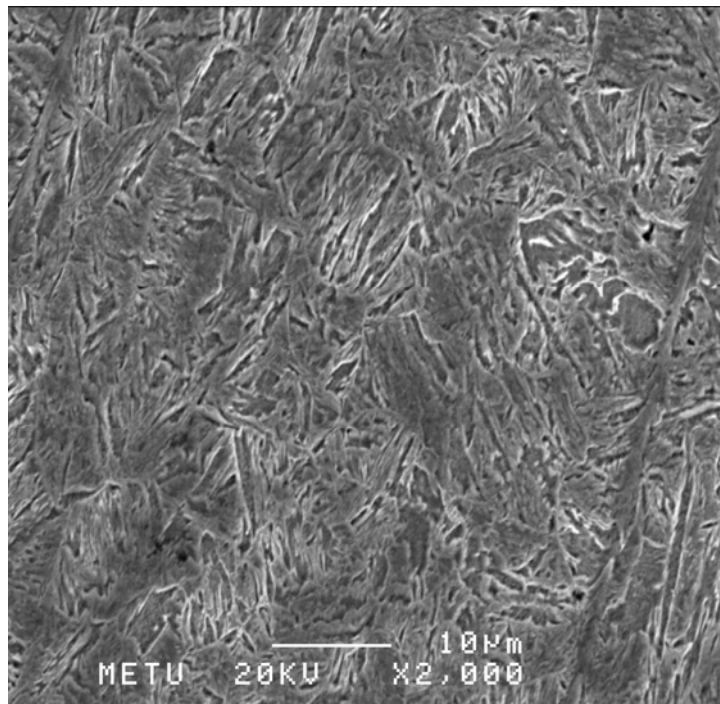


**Figure 7.6** Water quenched, 100% Martensite samples

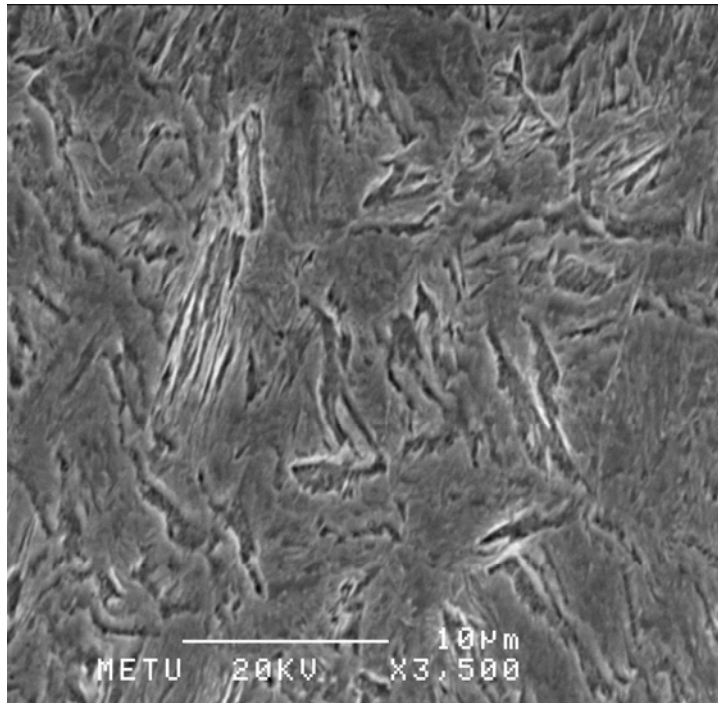
Figure 7.6 displays the fully martensitic structures consisting of martensite plates and some unresolved regions displaying no regular pattern. These plates are randomly oriented and different in length and thickness, in accordance with martensitic transformation in steels.

#### 7.4.1 Microstructures obtained after austempering at 300 °C

The empirical formulas given in chapter 5 and the examination of the reference TTT diagram used in this study reveals that the martensite start temperature of the steel is around 280 °C. Therefore, lower bainite is expected to grow at 300 °C. As in figure 7.7 and 7.8, 1 minute isothermal transformation at 300 °C reveals both bainitic and martensitic structures. Figure 7.8 is better evidence to elongated shape bainite sheaves which are free to lengthen without hindrance at this stage of the transformation. However, the comparison of the following figures with the reference martensite images given above reveals that the isothermally transformed structures contain a great amount of martensite. This is consistent with the mechanical values interpreted above. Toughness is relatively low and hardness is relatively high due to the presence of martensite.

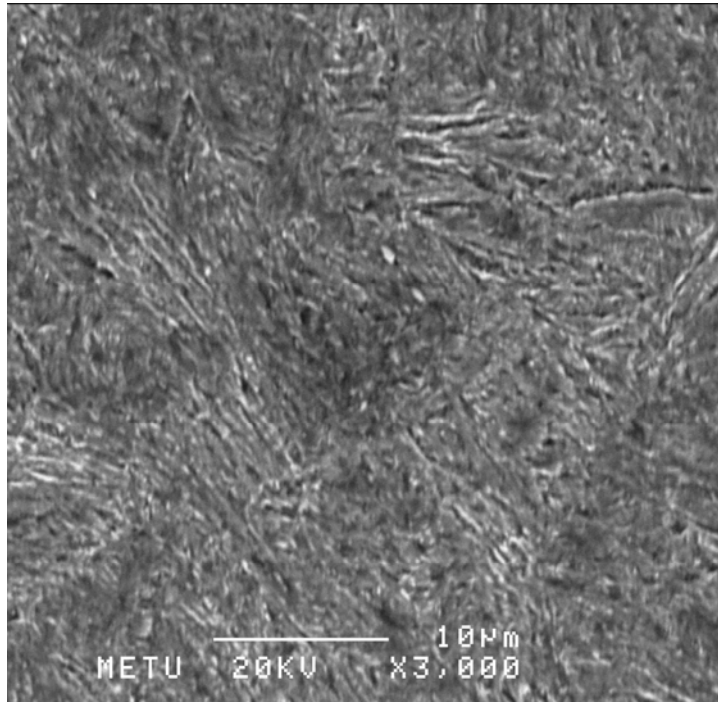


**Figure 7.7** Microstructure obtained after austempering at 300 °C for 1 min.  
(SEM Image)



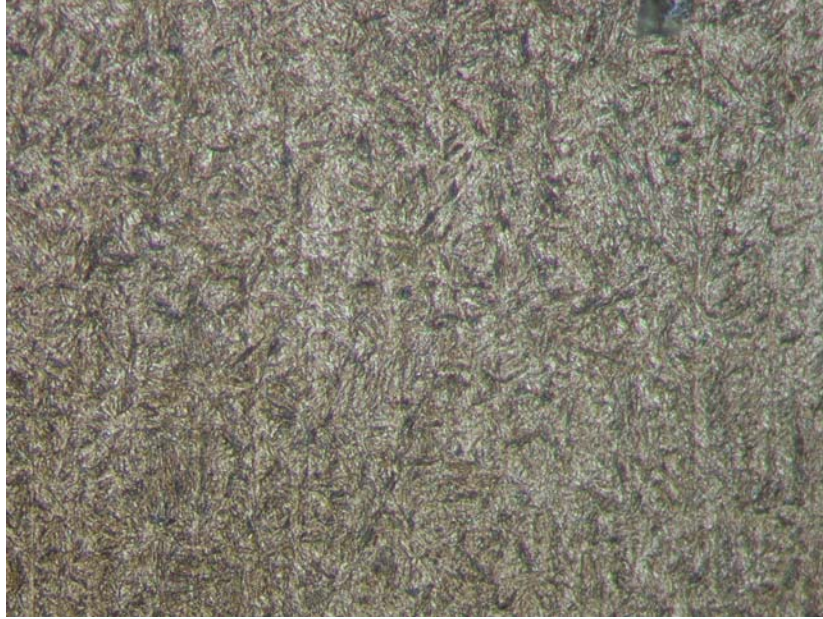
**Figure 7.8** Microstructure obtained after austempering at 300 °C for 1 min.  
(SEM Image)

Figure 7.9 shows the structure obtained after 10 minutes of transformation. The transformation product seen is partially bainitic and partially martensitic. Bainite sheaves grow parallel to each other and appear as long finger like parallel forms, both light and dark. Martensite also forms because the specimen is quenched after 10 minutes. The only difference of figure 7.9 from the above others is that the microstructure coarsens and parallel array of sheaves turn into non-parallel structure. The mechanical tests also revealed that there is not much difference between 1 minute and 10 minutes transformed products in terms of hardness and impact toughness which means that structures obtained should almost be the same. Microstructural evidence reveals this as well. According to mechanical test results and the discussion made before, the amount of bainite should be less than the amount of martensite. Images reveal, consequently, shapes that resemble typical bainite and also martensite.

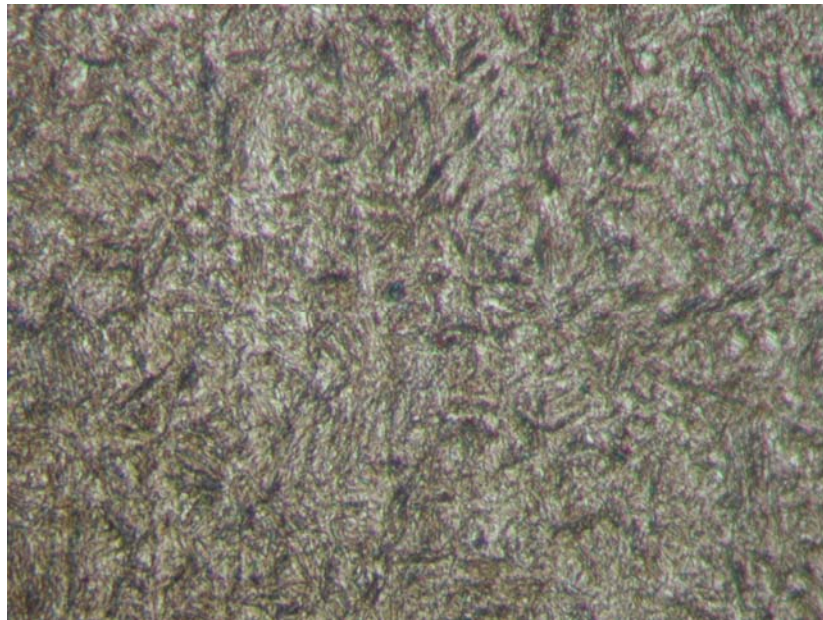


**Figure 7.9** Microstructure obtained after austempering at 300 °C for 10 min.  
(SEM Image)

Figures 7.10 and 7.11, which were taken by optical microscopy, display the acicular shaped bainitic structure. Although it is hard to distinguish between bainite and martensite at this resolution, bainite is the main constituent here. Long transformation time made the structure deformed and lost its sheaf shape.



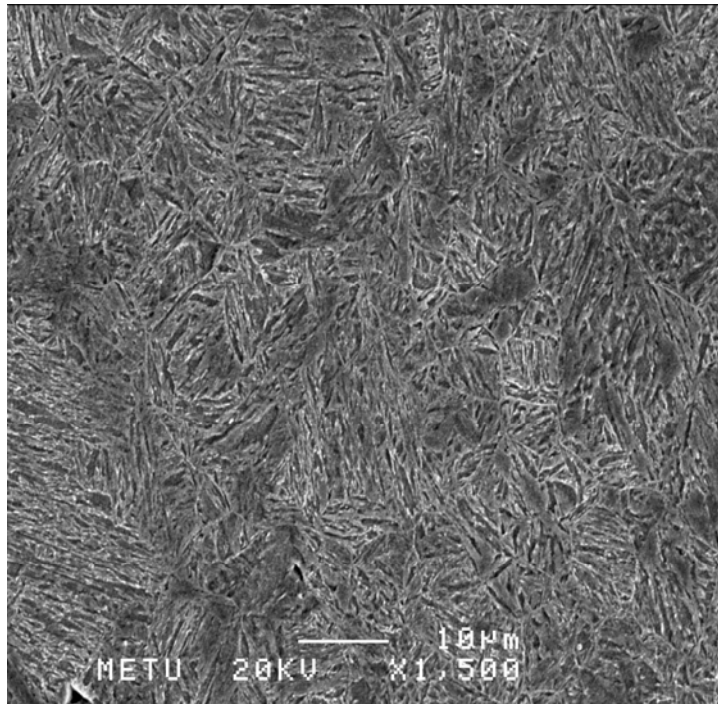
**Figure 7.10** Microstructure obtained after austempering at 300 °C for 10 hours.  
(Optical microscope image, ×960 magnification)



**Figure 7.11** Microstructure obtained after austempering at 300 °C for 10 hours.  
(Optical microscope image, ×2400 magnification)

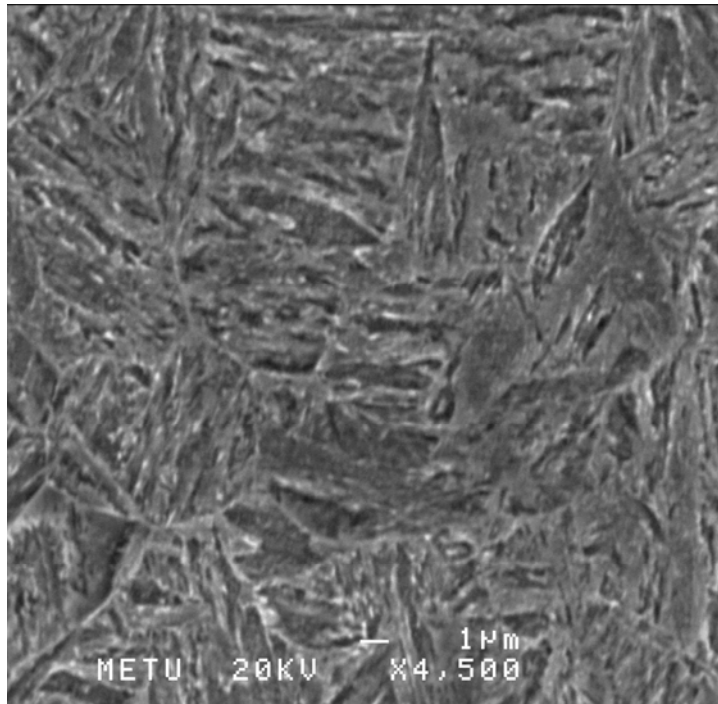
#### 7.4.2 Microstructures obtained after austempering at 325 °C

Figure 7.12 displays a mixed structure of bainite and martensite that is obtained after austempering at 325 °C for 1 minute. The image is a good visualization of lower bainite. It is easy to comment here that, the typical bainitic structures are more common here as compared to figures 7.7 and 7.8. Mechanical tests revealed the same with higher toughness values than the specimens transformed at 300 °C for 1 minute.

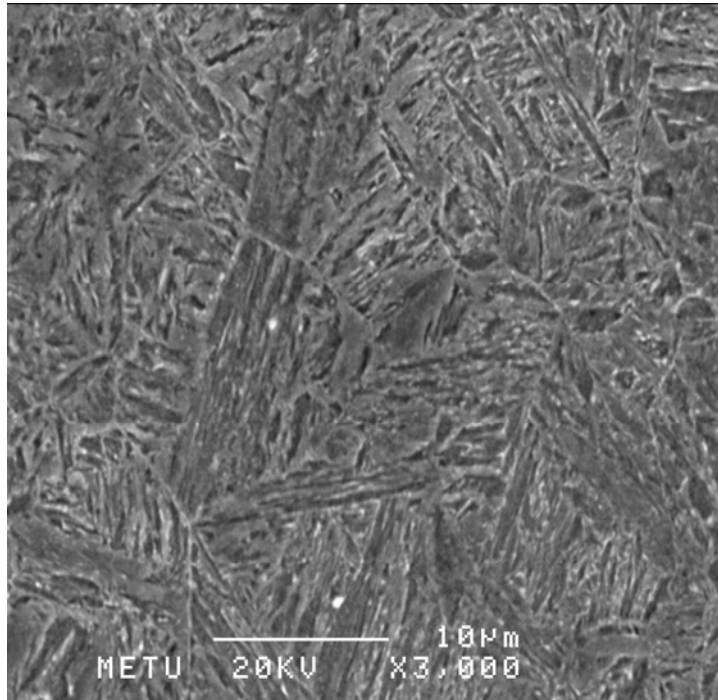


**Figure 7.12** Microstructure obtained after austempering at 325 °C for 1 min.  
(SEM Image)

Figures 7.13 and 7.14 have higher magnifications and display sheaves of bainite closer and clearer. Typical bainitic structures are easy to distinguish in these two images. Martensitic structures are also present and distinguishable. Especially figure 7.13 displays the finger-like bainitic sheaves covering the majority of the image. The much higher impact toughness values obtained at 325 °C for 1 minute is now easier to understand due to higher proportion of bainite observed as compared to samples transformed at 300 °C for 1 minute.

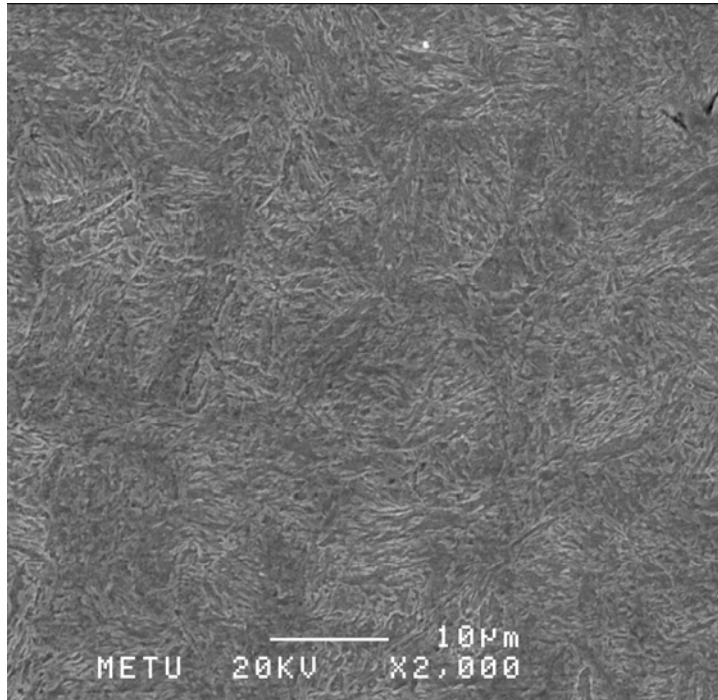


**Figure 7.13** Microstructure obtained after austempering at 325 °C for 1 min.  
(SEM Image)



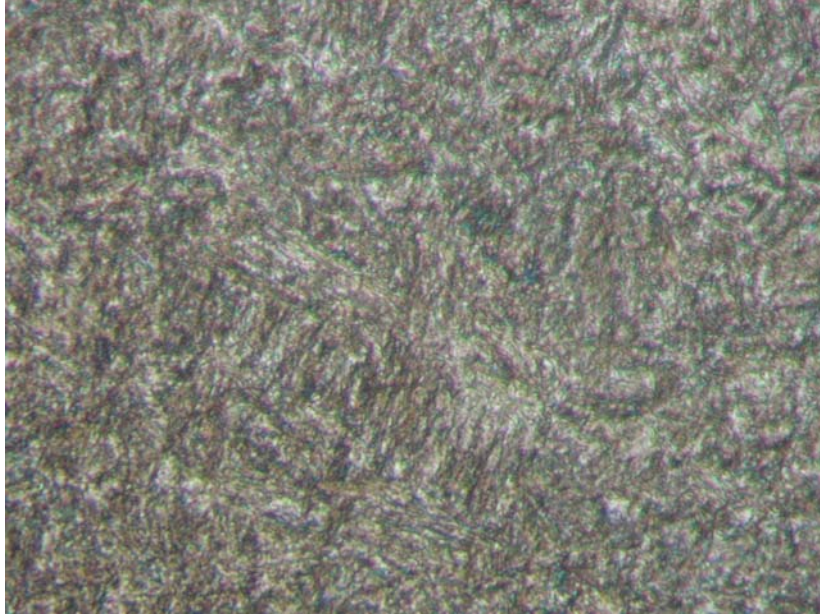
**Figure 7.14** Microstructure obtained after austempering at 325 °C for 1 min.  
(SEM Image)

Figure 7.15 illustrates the structure after 10 minutes of transformation. Elongated bainite sheaves and martensite plates are seen although it is hard to distinguish. TEM study is required to decide on the exact structures and allocate between bainite and martensite. The deformed structure and relatively lost sheaf shape as compared to shorter transformation times is observable here.



**Figure 7.15** Microstructure obtained after austempering at 325 °C for 10 minutes.  
(SEM Image)

Figures 7.16 and 7.17 shows the microstructure obtained after 10 hours. Bainitic structure degenerated at this transformation period although finger-like parallel bainitic structure is still observable. Coarsening is observed.



**Figure 7.16** Microstructure obtained after austempering at 325 °C for 10 hours.  
(Optical microscope image, ×2400 magnification)

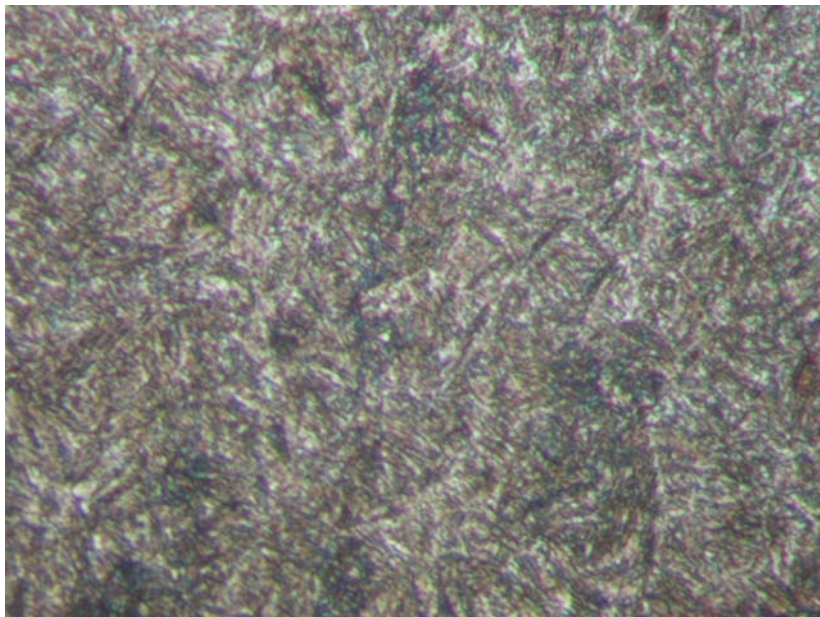


**Figure 7.17** Microstructure obtained after austempering at 325 °C for 10 hours.  
(Optical microscope image, ×3200 magnification)

### 7.4.3 Microstructures obtained after austempering at 350 °C

Figures 7.18-7.21 show the structure obtained at 350 °C after 1 minute transformation. Figure 7.18 displays the mixed structure of bainite and martensite. Figures 7.19-7.21 magnify the bainitic structures mixed with martensite. Typical lower bainitic structures are easy to distinguish.

Regarding the results of the mechanical tests, it is conclusive that the below structure contains the highest amount of bainite as compared to its counterparts at 300 °C and 325 °C. Easily observable bainitic structures in the following images are good evidence to this. Accompanying martensite and some untransformed regions are also observable.

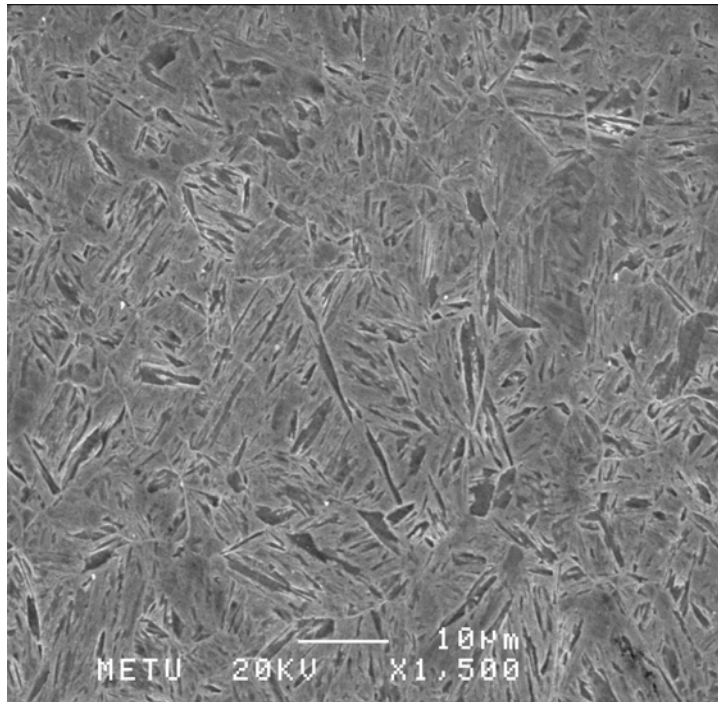


**Figure 7.18** Microstructure obtained after austempering at 350 °C for 1 minute.  
(SEM Image)

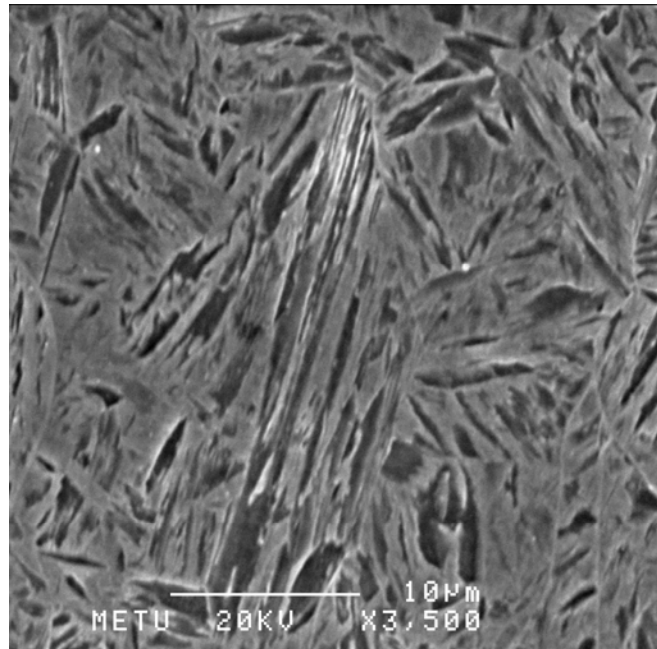


**Figure 7.19** Microstructure obtained after austempering at 350 °C for 1 minute.  
(SEM Image)

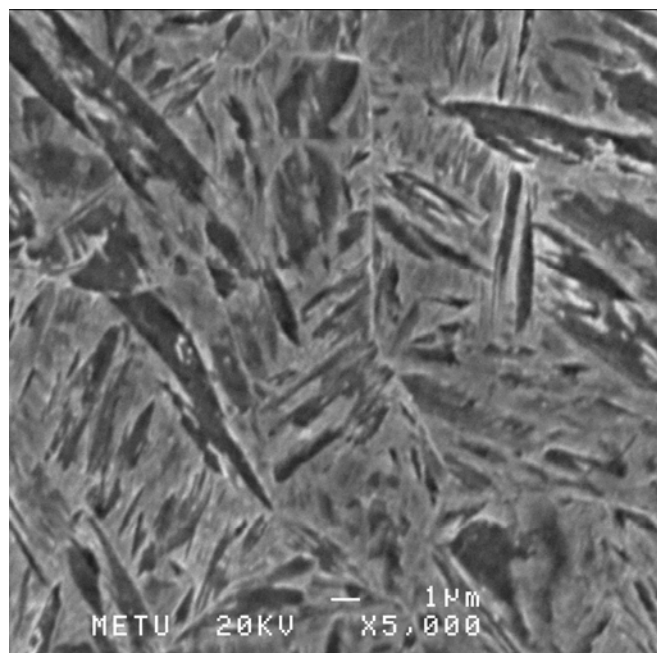


**Figure 7.20** Microstructure obtained after austempering at 350 °C for 1 minute.  
(SEM Image)

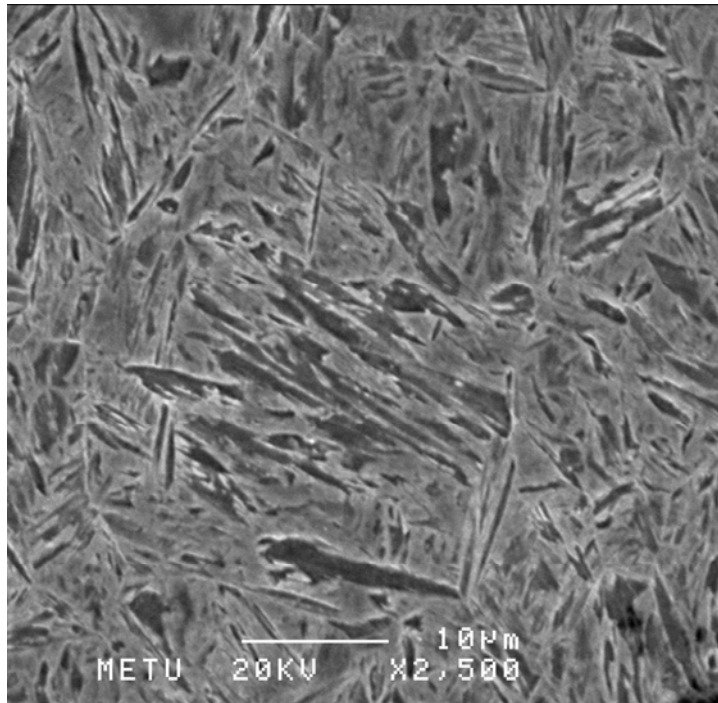


**Figure 7.21** Microstructure obtained after austempering at 350 °C for 1 minute.  
(SEM Image)

Figures 7.22 - 7.24 show the microstructure transformed at 350 °C for 10 hours. Although bainitic structures are distinguishable, the images do not provide clear shapes of bainite. Due to prolonged transformation times, bainitic structures are deformed and lost its sheaf shape almost completely. Coarsening occurred.

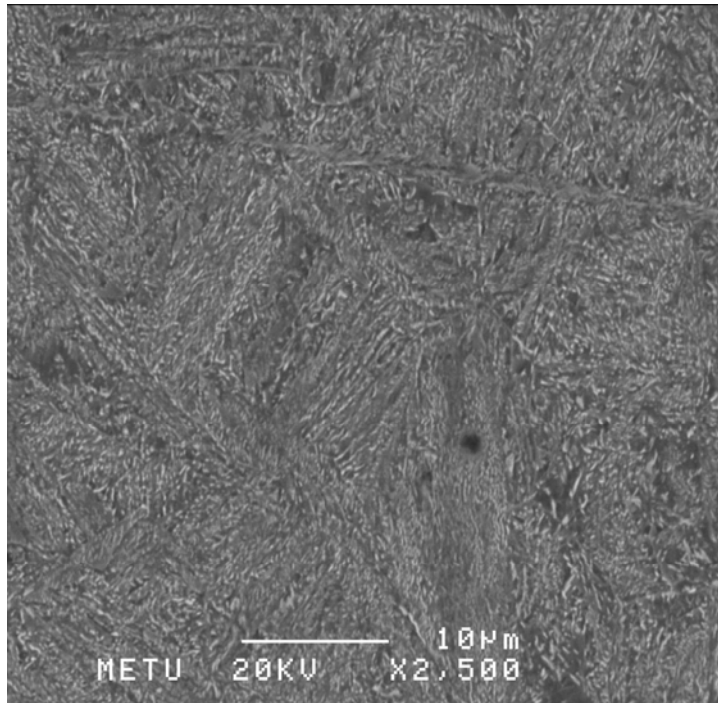


**Figure 7.22** Microstructure obtained after austempering at 350 °C for 10 hours.  
(SEM Image)

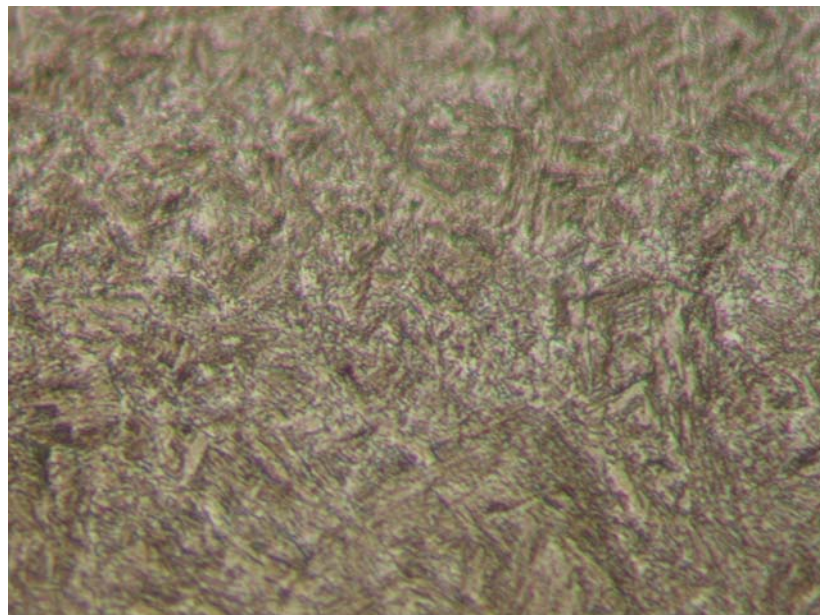


**Figure 7.23** Microstructure obtained after austempering at 350 °C for 10 hours.  
(Optical microscope image, ×2400 magnification)

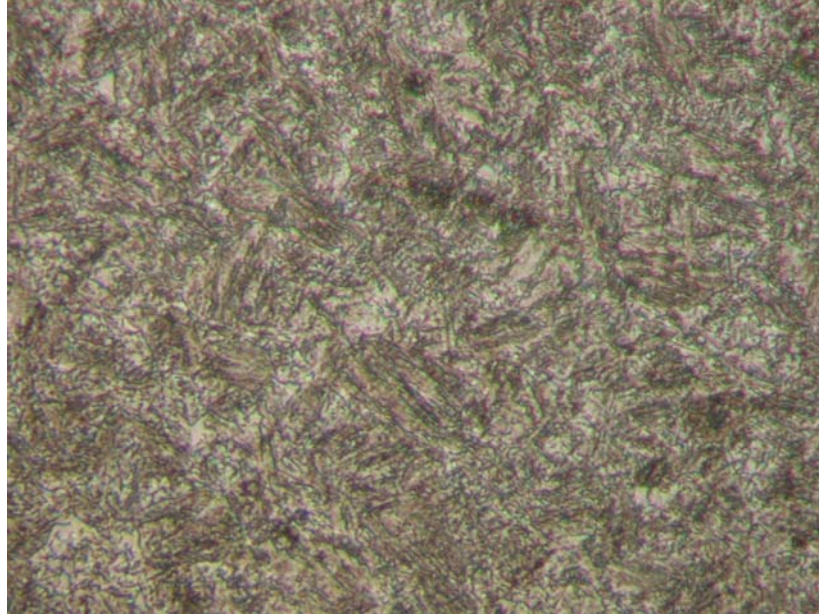


**Figure 7.24** Microstructure obtained after austempering at 350 °C for 10 hours.  
(Optical microscope image, ×2400 magnification)

The main microstructure obtained in this study is lower bainite. Microstructures analyzed reveal that majority of the structure is bainite; however, martensitic formations are always present almost in every microstructure analyzed. At prolonged transformation periods, coarsening occurred and bainitic sheaves lost their shapes. Images obtained provided good evidence for the results of the mechanical tests.

Although a similar study by Kurtulus [34] revealed rounded islands of bainite, especially in the lower temperature transformation products, such a structure was not observed in this study. Spanos et. al. [45], Reynolds et. al. [46] and Goldenstain and Aaronson [47] have reported similar nodular bainitic structures in isothermally transformed Mn, Mo or Cr alloyed steels with different carbon ratios. Although such formations have not been observed, TEM study would have revealed nodular bainitic structures in this study as well.

## CHAPTER 8

### CONCLUSION

The effect of austempering on mechanical properties of gun barrels is investigated in this study. Different austempering temperatures and different austempering periods revealed different microstructures and mechanical properties.

The following conclusions can be drawn from this study:

1. All three austempering temperatures produced bainitic structures. However, it is observed that even longest austempering times at all temperatures contain martensite.
2. Highest impact toughness values are measured at 300 °C and 325 °C for 1 hour isothermal holding period.
3. Hardness decreased with increasing austempering time. On the other hand, as isothermal transformation temperature increased, it was observed that hardness values decreased.
4. The best mechanical properties are achieved when the parts austempered for 1 hour at 325 °C.

5. Regarding impact toughness, it is observed that conventional quenching and tempering produced tougher structures at the same hardness level than austempering does. Machining problems faced during the preparation of samples might have had an influence.
  
6. Fracture toughness tests of austempered samples revealed structures with lower toughness than conventionally treated samples.

## REFERENCES

- [1] Krauss, G., Steels: Heat Treatment and Processing Principles, 1<sup>st</sup> printing, (1989)
- [2] \_\_\_\_\_, “Austempering”, Metals Handbook, 9<sup>th</sup> Edition, Vol. 4, (1981)
- [3] Smith, W. F., Structure and Properties of Engineering Alloys, McGraw-Hill Publishing Co., (1981)
- [4] The Mond Nickel Company Limited, Transformation Characteristics of Nickel Steels, (1952)
- [5] Bhadeshia, H. K. D. H., Bainite in Steels, 2<sup>nd</sup> Edition, (2001)
- [6] Irvine, K. J. and Pickering, F. B. JISI **201**, 518-531, (1963)
- [7] Knott, J. F. and Cottrell, A. H. JISI **201**, 249-260, (1963)
- [8] Knott, J. F. JISI **204**, 104, (1966)
- [9] Ritchie, R. O., Knott, J. F. and Rice, J. R. J. Mech. Phys. Sol. **21**, 395-400, (1973)
- [10] Knott, J. F. Advances in the Physical Metallurgy and Applications of Steels, Metals Society, London, 181, (1981)
- [11] Bowen, P., Druce, S. G. and Knott, J. F. Acta Metallurgica **34**, 1121-1131, (1986)
- [12] Parker, R. F. Metallurgical Transactions, **8A**, 1025, (1977)
- [13] Cao, W. D., Lu, X. P., Metallurgical Transactions, **18A**, 1567, (1987)
- [14] Naylor, J. P. and Krahe, P. R. Metallurgical Transactions, **5**, 1699-1701, (1974)

- [15] Pickering, F. B. Transformations and Hardenability in Steels, Climax Molybdenum, Ann Arbor, USA, 109-132, (1967)
- [16] Brozz, P., Buzzichelli, G., Mascanzoni, A. and Mirabile, M. Metal Science, **11**, 123-129, (1977)
- [17] Edmonds, D. V. and Cochrane, R. C. Metallurgical Transactions, **21A**, 1527, (1990)
- [18] Tomita, Y. and Okabayashi, K. Metallurgical Transactions, **17A**, 1203, (1986)
- [19] Ohmori, Y., Ohtani, H. and Kunitake, T. Metal Science, **8**, 357, (1974)
- [20] Ohmori, Y., Ohtani, H. and Kunitake, Transactions ISIJ, **12**, 147 (1972)
- [21] Tomita, Y. Journal of Material Science, **27**, 1705 (1992)
- [22] Irvine, K. J. and Pickering, F. B. ISI Rep. 93, London, 110-125, (1965)
- [23] Lyman, T. and Troiano, A. R. Trans. ASM **37**, 402-448, (1946)
- [24] Kamada, A., Koshizuka, N. and Funakoshi, T. Trans. ISIJ **16**, 407, (1976)
- [25] Liu, C.D. and Kao, P.W., Material Science and Engineering, 510, 171, (1990)
- [26] Sandvik, B. P. J. and Nevalainen, H. P., Metals Technology, June, 231, (1981)
- [27] Baozhu, G., Krauss, G. Journal of Heat Treating, **4**, 365, (1986)
- [28] Tomita, Y., Okabayashi, K., Metallurgical Transactions, **14**, 485, (1983)
- [29] Tomita, Y., Okabayashi, K. Metallurgical Transactions, **14**, 2387, (1983)

- [30] Tomita, Y., Okabayashi, K. Metallurgical Transactions, **16**, 83, (1985)
- [31] Narasimha, T.V.L., Dikshit, S.N., Malakandaiah, G., Rao, P.R., Scripta Metallurgia, **24**, 1323, (1990)
- [32] Tomita, Y., Journal of Materials Science, **24**, 1357, (1989)
- [33] Joarder, A., Sarma, D.S., Materials Transactions JIM, **32**,705, (1991)
- [34] Kurtulus, B.M., M.S. Thesis, METU, 1994, 133 pages
- [35] Li, Z. and Wu, D., Effects of holding temperature for austempering on mechanical properties of Si-Mn TRIP steel, Journal Of Iron and Steel Research International 11 (6): 40-44, (2004)
- [36] Mirak, A.R. and Nili-Ahmadabadi, M., Effect of modified heat treatments on the microstructure and mechanical properties of a low alloy high strength steel, Materials Science and Technology 20 (7): 897-902, (2004)
- [37] Putatunda, S.K., Influence of austempering temperature on microstructure and fracture toughness of a high-carbon, high-silicon and high-manganese cast steel, Materials & Design 24 (6): 435-443, (2003)
- [38] Putatunda, S.K., Austempering of a silicon manganese cast steel, Materials and Manufacturing Processes 16 (6): 743-762 (2001)
- [39] Li, Y.X. and Chen, X., Microstructure and mechanical properties of austempered high silicon cast steel, Materials Science and Engineering a-Structural Materials Properties Microstructure and Processing 308 (1-2): 277-282, (2001)
- [40] Putatunda, S.K., Fracture toughness of a high carbon and high silicon steel, Materials Science and Engineering a-Structural Materials Properties Microstructure and Processing 297 (1-2): 31-43 JAN 15 2001
- [41] Lee, Sunghak, PhD Thesis, Correlation of Microstructure and Fracture Toughness in two 4340 Steels (TME), Brown University, 132 pages; AAT 8617591 (1986)

- [42] Nehrenberg, A. E., In Contribution to Discussion on Grange and Stewart, Trans. Amer. Inst. Min. Met. Engrs., vol.167, pp 494-498, (1946)
- [43] Grange, R. A. and Stewart, H. M., Metals Technology, (1946)
- [44] Naylor, J. P., Metallurgical Transactions, **10**, 861, (1979)
- [45] Spanos, G., Farg, H. S., Sarmo, D. S., Aaronson, H. I., Material Transformation, **21A**, 1397 (1990)
- [46] Reynolds, W. T., Li, I. Z., Shui, C. K., Shiplet, G. J., Aaronson, H. I., Phase Transformations, **8**, 994, (1992)
- [47] Goldenstain, H. and Aaronson, H. I., Metallurgical Transactions, **21A**, 1397, (1990)
- [48] Chang, L. C. and Bhadeshia, H. K. D. H., Microstructure of lower bainite at large undercoolings below bainite start temperature, Materials Science and Technology, vol.12, (1996)
- [49] Bhadeshia, H. K. D. H., PhD Thesis, Cambridge University, (1979)
- [50] Bhadeshia, H. K. D. H. and Edmonds, V., Metall. Transactions, **10A**, 895, (1979)
- [51] Padmanabhan, R. and Wood, W. E., Materials Science and Engineering, 66, 1, (1984)
- [52] FORTRAN Program, MAP\_STEEL\_MUCG46, Materials Algorithms Project Program Library, Provenance of Source Code: H.K.D.H. Bhadeshia, Phase Transformations Group, Department of Materials Science and Metallurgy, University of Cambridge, Cambridge, U.K.
- [53] Erinc, M. Master Thesis, METU, (2003)

## APPENDIX

All impact toughness and hardness measurements are as follows.

For 300 °C:

	<b>1 min</b>	<b>T (J)</b>	<b>Avg. T (J)</b>	<b>HRC 1</b>	<b>HRC 2</b>	<b>HRC 3</b>	<b>Avg. HRC</b>	<b>Overall Avg. HRC</b>
<b>Spec. no.</b>								
<b>20</b>	CX1	7	<b>15.67</b>	55.7	56	55.5	55.73	<b>54.52</b>
<b>30</b>	BY8	13		52.3	52.6	52.9	52.60	
<b>20</b>	AX3	27		54	54.7	57	55.23	
	<b>10 min</b>							
<b>20</b>	BY1	7.5	<b>15.67</b>	57.2	55.7	56.8	56.57	<b>56.28</b>
<b>30</b>	BX7	12.5		54.9	55.4	54.6	54.97	
<b>20</b>	AY4	27		58.2	56.4	57.3	57.30	
	<b>1 hr</b>							
<b>20</b>	AX2	30.5	<b>26.50</b>	48.4	47.1	48.2	47.90	<b>48.11</b>
<b>30</b>	CY5	24		47.9	48.4	48.2	48.17	
<b>20</b>	BY4	25		47.8	48.6	48.4	48.27	
	<b>10 hr</b>							
<b>20</b>	BY2	20	<b>17.67</b>	47.4	47.6	46.4	47.13	<b>46.93</b>
<b>30</b>	CX5	16		47.1	47.2	47.3	47.20	
<b>20</b>	BX4	17		46.5	46.5	46.4	46.47	

For 325 °C:

	<b>1 min</b>	<b>T (J)</b>	<b>Avg. T (J)</b>	<b>HRC 1</b>	<b>HRC 2</b>	<b>HRC 3</b>	<b>Avg. HRC</b>	<b>Overall Avg. HRC</b>
<b>Spec. no</b>								
<b>30</b>	AX1	24.5	<b>22.67</b>	54.7	54.4	54.5	54.53	<b>53.40</b>
<b>20</b>	BY7	21.5		53.3	52.7	53.5	53.17	
<b>30</b>	CY3	22		52.6	52.4	52.5	52.50	
	<b>10 min</b>							
<b>30</b>	BY1	21	<b>24.50</b>	52	50.9	52.1	51.67	<b>52.01</b>
<b>20</b>	AY7	30.5		53.8	53.5	53.5	53.60	
<b>30</b>	AX3	22		50.3	51	51	50.77	
	<b>1 hr</b>							
<b>30</b>	CY1	23.5	<b>25.83</b>	45.4	45.8	45.2	45.47	<b>45.33</b>
<b>20</b>	AX7	27		45.5	46.1	45.1	45.57	
<b>30</b>	AY4	27		45.3	44.8	44.8	44.97	
	<b>10 hr</b>							
<b>30</b>	AY1	22	<b>19.67</b>	44.1	45.6	44.1	44.60	<b>44.28</b>
<b>20</b>	BX7	21		44.2	44.4	43.2	43.93	
<b>30</b>	BX4	16		44.4	44.5	44	44.30	

For 350 °C:

	<b>1 min</b>	<b>T (J)</b>	<b>Avg. T (J)</b>	<b>HRC 1</b>	<b>HRC 2</b>	<b>HRC 3</b>	<b>Avg. HRC</b>	<b>Overall Avg. HRC</b>
<b>Spec. no</b>								
<b>20</b>	AX1	20	<b>27.67</b>	53.8	53	52.2	53.00	<b>53.90</b>
<b>30</b>	BY7	33		53.9	53.5	53.5	53.63	
<b>20</b>	CX3	30		54.9	55.6	54.7	55.07	
	<b>10 min</b>							
<b>20</b>	BX1	24	<b>23.00</b>	52.2	52.4	52.6	52.40	<b>52.27</b>
<b>30</b>	BX8	20		52	51	51.2	51.40	
<b>20</b>	CY3	25		52.1	53.8	53.1	53.00	
	<b>1 hr</b>							
<b>20</b>	AY1	21	<b>17.33</b>	44.9	46.1	43	44.67	<b>44.29</b>
<b>30</b>	AX7	18		43.8	42.5	43.1	43.13	
<b>20</b>	BY3	13		45.2	43.8	46.2	45.07	
	<b>10 hr</b>							
<b>20</b>	CY1	12	<b>16.83</b>	41.8	41.9	41.9	41.87	<b>41.64</b>
<b>30</b>	AY6	18.5		41.1	40.4	40.7	40.73	
<b>20</b>	AX4	20		42.7	42	42.3	42.33	